Renewable and Sustainable Energy Reviews 73 (2017) 408–422

Contents lists available at ScienceDirect

Renewable and Sustainable Energy Reviews

journal homepage: www.elsevier.com/locate/rser

A review of materials selection for optimized efficiency in quantum dot sensitized solar cells: A simplified approach to reviewing literature data

Ijaz A. Rauf[a,b,*], Pouya Rezai[c]

[a] SolarGrid Energy Inc. 9131 Keele Street, Suite A4, Vaughan, Ontario, L4K 0G7 CANADA
[b] Department of Physics and Astronomy, 128 Petrie Science and Engineering Building, York University, 4700 Keele Street, Toronto, Ontario, Canada M3J 1P3
[c] Department of Mechanical Engineering, Lassonde School of Engineering, York University, 4700 Keele Street, Toronto, Ontario, Canada M3J 1P3

ARTICLE INFO

Keywords:
Solar cells
Analysis of reviewed data
Inferential statistics application
Photovoltaic materials
Liquid electrolyte solar cells
All solid state solar cells

ABSTRACT

Quantum dot (QD) sensitized solar cells have been receiving significant attention because of their potential to replace the existing conventional solar cells as low cost and high efficiency alternatives. This widespread attention has generated a large number of published research papers in the field that were recently reviewed. The challenge in reviewing the literature is in transforming the collected technical information generated through independently conducted perturbation experiments into an alternative point of view. A unique approach based on inferential statistics is explained and applied to reviewed QD based solar cells data. Analyzing the data in this fashion has provided us new and previously unknown insight into the operation and functioning of solar cells as well as the relative quantitative importance of each variable involved in determining the properties of interest in solar cells. This methodology is very powerful and can be applied to gain insight through reviewing the published data in any field of science to set the direction for ongoing and future research. In addition, the response surface methodology is explained and used to predict the reachable optimum efficiency of 20% with a given set of materials combination given the current state of the art.

1. Introduction

The world now uses energy at a rate of approximately 15 trillion watts (TW) [1]; this demand is expected to more than double by 2050, even with aggressive conservation and energy efficiency measures [2]. Incremental improvements in existing energy networks will not be adequate to supply this demand in a sustainable way. Pressure on existing networks is bound to raise energy costs; this coupled with the threat of global warming has triggered a widespread interest in renewable energy. The challenge in adopting the photovoltaic technology as the primary source of power generation on a global scale is dramatically reducing the cost/watt of delivered solar electricity — by approximately a factor of 5–10 to compete with fossil and nuclear electricity and by a factor of 25–50 to compete with primary fossil energy. Scientists around the world are working on bringing these costs down. This can be done in two ways; reducing the cost of manufacturing/materials and/or improving the efficiency of the devices.

Over the last decade QDs sensitized and most recently heterojunction perovskite solar cells (schematically shown in Fig. 1) have attracted widespread attention [3–5]. In these solar cells, QDs or perovskite materials act as the absorber of sunlight and thus electron/hole pairs are generated in them. The wide bandgap semiconductor collects the electrons while the electrolyte or the hole transport material removes holes from the QD. Most of the published literature for these solar cells has recently been reviewed from various perspectives, such as, materials synthesis techniques, material types (sensitizer and wide bandgap semiconductor (WBGS) materials and their combination), solar cell architecture, charge transport, energy band alignment, electrolyte type and the counter electrode materials [3,6–12]. Review articles of good quality are frequently needed given the existence of ever growing number of research papers in this field. These review articles are expected to provide a detailed synthesis of the findings of reviewed research contributions, examine the current state of the science, initiate discussions about the research methodologies and the findings and set the stage for ongoing and future research. The real challenge in reviewing the literature is in transforming independently collected technical information generated through individually conducted controlled perturbation experiments into an alternative point of view. The information generated may contain undefined or not well understood relations amongst a multitude of system variables.

The task is further complicated by the fact that the numerous attempts to understand the dependence of semiconductor sensitized

* Corresponding author at: SolarGrid Energy Inc. 9131 Keele Street, Suite A4, Vaughan, Ontario, L4K 0G7 CANADA.
E-mail addresses: irauf@solargridenergy.ca, iarauf@yorku.ca (I.A. Rauf), prezai@yorku.ca (P. Rezai).

http://dx.doi.org/10.1016/j.rser.2017.01.137
Received 27 June 2016; Received in revised form 9 December 2016; Accepted 19 January 2017
Available online 31 January 2017
1364-0321/

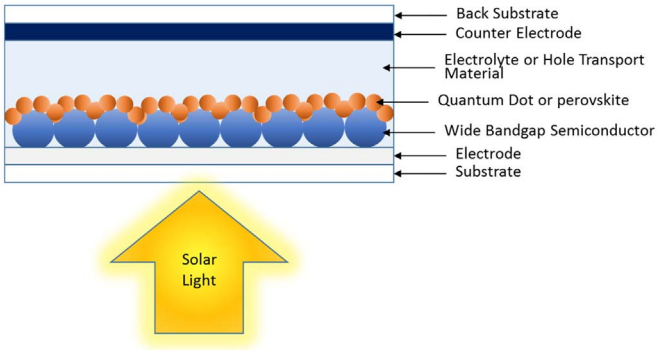

Fig. 1. Schematics of a typical quantum dot sensitized or a perovskite solar cell.

solar cell material properties based on the processing parameters in the literature reviewed so far had involved traditional "One variable at a time (OVAT)" methodology to experimentation. Although some qualitative indications of the combined effects and importance of optimizing the combination of a variety of variables has been made in the literature based on the OVAT experimentation, no quantitative information is found on the relative importance of each of the above-mentioned factors and their combined effects (interactions) on the solar cell performance.

Inferential statistical analysis of reviewed experimental data can play a pivotal role in transforming the observed data into critical information for the advancement of underlying science and accelerated achievement of the research goals in the field of interest. Doing more with less has always been the central theme within the scientific research community. The recent drastic funding cuts for basic research because of recession have initiated a discussion among the academic and research community to develop and utilize methodologies for faster advancement of systems knowledge at minimal costs [13–15]. Different approaches have been utilized in biomedical sciences [16,17] but never formalized with the theoretical framework for historical data analyses in solar cell materials. In this paper, we present a unique methodology to provide systems view of liquid electrolyte QD and all solid state solar cells (ASSSCs) based on the inferential statistics. This method is applied to literature data we collected and reviewed.

2. Theory behind methodology

Simple example of a linear relationship between an input variable and an outcome is given by the following equation:

$$y = \mathrm{ax} + b + \varepsilon, \tag{1}$$

where a and b are constants (a being the slope and b being the y-intercept) and ε represents the error.

If an experimenter wants to study this relationship and has resources to perform only 4 experiments, a scientist would choose to make one measurement at four levels spanning the region of interest. This does not allow the quantification of the error at each of the points and does not establish if the changes observed are due to changes in the experimental variables or caused by the measurement error (or variation). From statistical point of view, the best strategy would be to perform two experiments at 2-levels with one repeat each giving a total of 4 experiments, providing an ability to gather much more information for decision making.

The relationship between the output (or dependent) variable 'y' and input (or natural) variables 'z' especially when y is dependent on more than one variables can be expressed as:

$$y = f(z_1,\ z_2,\ z_3,\ \ldots..z_n,\ ) + \varepsilon \tag{2}$$

where f is an unknown function, which may be very complicated, and ε represents other non-systematic sources of variability not accounted for in the function f, such as measurement error. The goal is to approximate f by a relatively simple analytical function based on experimental data. The variables z_1, z_2 .... z_n are natural variables (for example, time & temperature in a synthesis experiment) that are measured in units used in the experiments (for example, seconds for time and °C or °K for temperature etc).

For performing analyses using inferential statistical tools, the natural variables (or the assigned arbitrary variables) are converted into dimensionless coded variables x_1, x_2, ... x_n on a scale of −1 (the lowest value) to +1 (the highest value) as follows:

$$x_n = \frac{z_i - (z_{+1} + z_{-1})/2}{(z_{+1} - z_{-1})/2} \tag{3}$$

This converts all variables in a study to a common scale and allows evaluation of the impact of each variable and its interaction on the outcome independent of its measurement units. The simplest model of the response surface can be approximated by multiple linear regression as an extension of Eq. (1) with 'n' input variables as follows:

$$y_i = b_0 + \sum_{j=1}^{n} b_j x_{ij} + \varepsilon \tag{4}$$

Where the linear regression coefficients, b_j, are estimated from the experimental data through model fitting. When the change in the output variable due to a change in an input variable x_j depends on the values of other variables, this can be expressed as:

$$y_i = b_0 + \sum_{j=1}^{n} b_j x_j + \sum_{i=2}^{n} \sum_{j=1}^{i-1} b_{ij} x_i x_j + \varepsilon \tag{5}$$

Here the term $b_{ij}x_ix_j$ represents the statistical interaction between variable x_i and x_j. Both Eqs. (4) and (5) are linear terms and thus represent the first order model. The relationship between variables may not always be linear and a more complex model may need to be developed. If a strong quadratic relationship is expected this can be expressed as a 2nd order model:

$$y_i = b_0 + \sum_{j=1}^{n} b_j x_j + \sum_{i=2}^{n} \sum_{j=1}^{i-1} b_{ij} x_i x_j + \sum_{j=1}^{n} b_{jj} x_j^2 + \varepsilon \tag{6}$$

Parameters b are often estimated from experimental data using computation software designed for this purpose and are donated by $\hat{b}$. The values predicted by (4) for $\hat{y}_i$ based on the input variables x_{i1}, x_{i2} ... x_{in} is given as:

$$\hat{y}_i = \hat{b}_0 + \sum_{j=1}^{n} \hat{b}_j x_{ij} + \varepsilon \tag{7}$$

Similarly, the values predicted for Eqs. (5) and (6) based on input variables x_{i1}, x_{i2} ... x_{in} are given as:

$$\hat{y}_i = \hat{b}_0 + \sum_{j=1}^{n} \hat{b}_j x_j + \sum_{i=2}^{n} \sum_{j=1}^{i-1} \hat{b}_{ij} x_i x_j + \varepsilon \tag{8}$$

And

$$\hat{y}_i = \hat{b}_0 + \sum_{j=1}^{n} \hat{b}_j x_j + \sum_{i=2}^{n} \sum_{j=1}^{i-1} \hat{b}_{ij} x_i x_j + \sum_{j=1}^{n} \hat{b}_{jj} x_j^2 + \varepsilon \tag{9}$$

The difference between observed and predicted values is called residual and is useful in making inferences about the adequacy of the model. The residuals are calculated as:

$$\hat{\varepsilon}_i = y_i - \hat{y}_i \tag{10}$$

2.1. Inference theory

There are two main limitations to the exploratory historical data analysis. One is that the data are usually only examined in "slices". For example, we can look at the pattern due to changes in a variable (and

the residual variability) ignoring blocks, and then look at the pattern due to blocks; but it is difficult to look at several components of the pattern at the same time. This is particularly important when there are many factors or when data structures are complicated as is the case in large historical datasets. We need a method of allocating variability across different sources all at once: this is the role of ANOVA. Still, the conclusions drawn from ANOVA are subjective. Some measure of precision needs to be attached to the individual effects observed. For this we need more formal methods of analysis, and usually a hypothesis test is used (two tail *t*-test in case of normal data) for the individual effects.

The simple linear model and the ANOVA model can be viewed as a case of a more general linear model where the variations of one variable y are explained by 'n' explanatory variables x_i respectively. An important application of this is the least squares fitting. The idea is to approximate 'y' by a linear combination of x_i, such that the model is the best fit of y in the least-squares sense. The method used to test this problem is to calculate (or obtain) the total variation and to decompose it into the sources of variation.

Total sum of the square residuals for a sample size of 'N' is used to calculate the variance in the system and is given as:

$$\text{Variance} = \quad s^2 = \frac{\sum_{i=1}^{n} \epsilon_i^2}{N-1} = \frac{\sum_{i=1}^{n} (y_i - \hat{y}_i)^2}{N-1} \tag{11}$$

Let's consider the example of a large set of data on solar cells with a sample size 'N' that we have collected from the literature. Within this dataset there are two groups (two levels), one group of 'K' solar cells that used absorber material 'A' while the other group of (N-K) solar cells used absorber material 'B', each with their own normal distributions (Fig. 2). In this case two more square residuals can be calculated for making inferences; that is, sum of squares between the distribution for the two absorber materials $SS_B=\sum_{i=1}^{n} n_i(\hat{y}_i - \hat{y})^2$and the sum of squares within the distribution from any given absorber material $SS_W=\sum_{i=1}^{a}\sum_{j=1}^{n} (y_{ij} - \hat{y}_i)^2$and $SS_E=\sum_{i=1}^{n} (y_i - \hat{y}_i)^2$. The total sum of squares for the overall distribution containing all solar cells is thus given as:

$$SS_T = \sum_{i=1}^{a}\sum_{j=1}^{n} (y_{ij} - \hat{y})^2 = SS_B + SS_W + SS_E \tag{12}$$

where, 'a'=the number of groups/levels, y_{ij}=the jth data point in the ith group, n_i=the number of data points in the ith group or level, $\hat{y}$=the grand mean, and $\hat{y}_i$=the mean of the ith group or level. Mean square variance total (MS_T), mean square variance between (MS_B) and mean square variance within (MS_W) can be calculated from Eq. (12) by dividing the sum of squares with the appropriate degrees of freedom:

$$\left.\begin{aligned} \text{MS}_T &= \frac{\sum_{i=1}^{a}\sum_{j=1}^{n}(y_{ij} - \hat{y})^2}{N-1} \\ \text{MS}_B &= \frac{\sum_{i=1}^{a}\sum_{j=1}^{n}(y_{ij} - \hat{y})^2}{K-1}, \\ \text{MS}_W &= \frac{\sum_{i=1}^{a}\sum_{j=1}^{n}(y_{ij} - \hat{y})^2}{N-K} \end{aligned}\right\} \tag{13}$$

If between the group variation is larger than within-the-group variation (i.e. $MS_B > MS_W$) then the most variation in 'y' is due to 'x', however, if between the group variation is smaller than the within group variation (i.e. $MS_B < MS_W$), variation in 'y' is due to things other than 'x'. The ANOVA determines if the differences between the averages of the levels is greater than the one that could reasonably be expected from the variation that occurs within a level. This could be extended to include multiple variables divided into blocks and ANOVA analyses could be used to test the validity of the model and the confidence level therein. F-statistic (critical value for F) and the model correlation coefficient R^2 are thus calculated from Eqs. (12) and (13) as:

$$F_0 = MS_B/MS_W \;\&\; R^2 = \frac{SS_B + SS_W}{SS_T} = 1 - \frac{SS_E}{SS_T} \tag{14}$$

The F-statistics could be used to calculate the confidence interval in accepting or rejecting the hypothesis for the validity of the overall medal. The correlation coefficient thus measures the percent total variability that can be explained by the variables included in the model. When applied to comparison of two averages, or an average and a known value (like in case of individual variables included in the model), ANOVA simplifies to what is called a *t*-test, which is based on a t-distribution.

Since observed differences in the response can either be due to the true effects of the change in the input variables, or due to the artefacts of the random variation, it is important to distinguish between these two situations. The statistical approach utilizing a hypothesis test based on t-statistics is the only objective way of making such conclusions from the data. The t-distribution is a symmetric probability distribution centered at zero, like the normal probability distribution. The difference is that the t-distribution has a variance that depends on the degrees of freedom of the standard error in the statistic of interest.

The t-distribution is used to determine t-statistic which is then used to calculate a confidence level for the true impact of the variable under consideration on the output or the dependent variable and is given as:

$$t_0 = \frac{\bar{y}_1 - \bar{y}_2}{S_p\sqrt{\frac{1}{N_1} - \frac{1}{N_2}}}, \tag{15}$$

where, pooled standard deviation $S_p = \sqrt{\frac{(n_1-1)S_1^2 + (n_2-1)S_2^2}{n_1+n_2-2}}$

The area under a t-distribution beyond the critical value of t_0 is donated by α. The t-statistic assigns a level of confidence (1-α) to our decision making in terms of including the given variable in our model or excluding it from the model (Fig. 3). In other words, we say that we want to have 1-α level of confidence that the given variable has a statistically significant effect on the output variable or property of interest. For example, at a 90% confidence level 1-α=0.90 and α=0.10, conventionally used levels are 90% (somewhat confident), 95% (fairly confident), and 99% (quite confident). Once an α value is selected based on the processes involved, statistical analyses are performed, calculating the actual area under the curve beyond t_0. This value is termed as p-value and is compared with α for including the term in the model or not.

Simply put, one tests the hypothesis: H_0:b_j=0 against H_1:b_j≠0. If the null hypothesis, H_0 is not rejected, there is no evidence that levels of

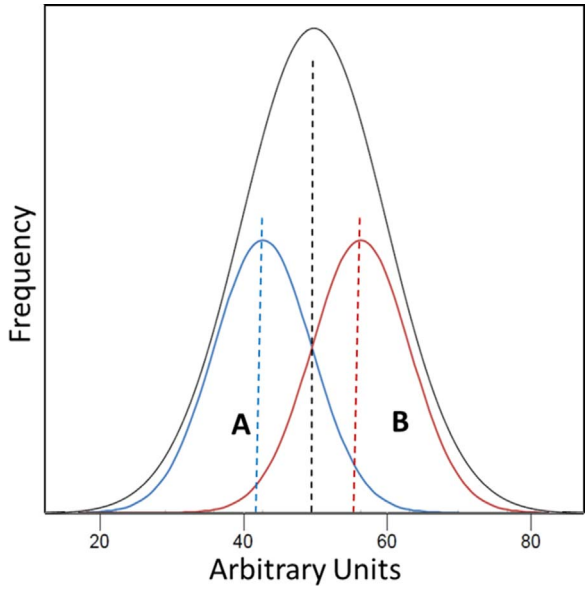

Fig. 2. Arbitrary normal distributions representing slice of data within a large normal dataset.

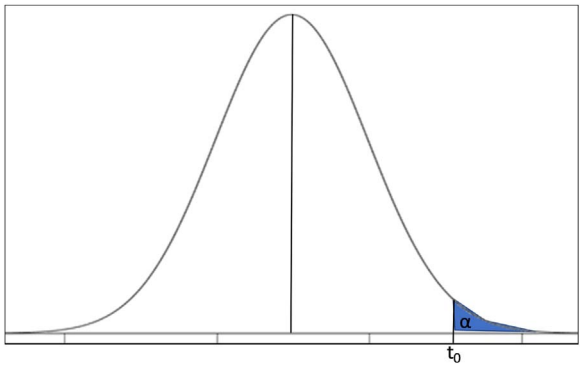

Fig. 3. A distribution showing area 'α' beyond the critical value of t_0 for calculating the level of confidence.

the input variable x_j result in systematic differences in the response, and the term can be excluded from the model. On the other hand, if H_0 is rejected, the corresponding term has a statistically significant effect and it should be kept in the model.

2.2. Response surface methodology (RSM)

Once a reasonably acceptable model based on the reviewed data is built using the theory & methodology given in the previous two subsections, RSM can be used to provide predictions for the optimization. The objective of the RSM is to optimize a response (output variable) which is influenced by several independent variables (input variables). Let's consider a simple case where the response variable 'y' is dependent only on two variables x_1 and x_2 then from Eq. (4) we obtain $y=f(x_1, x_2)+\varepsilon= b_O +b_1\times_1+b_2\times_2+\varepsilon$, the error term ε represents any measurement error on the response, as well as other type of variations not counted in *f*. However, if there is a curvature in the response surface, then a higher degree polynomial should be used. The approximating function with 2 variables is then a second-order model based on Eq. (6) and is given as:

$$y = b_0 + b_1x_1 + b_2x_2 + b_{11}x_1^2 + b_{22}x_2^2 + b_{12}x_1x_2 + \varepsilon \quad (16)$$

In general, all RSM problems use either one or the mixture of both models, especially when the response variable is dependent on multiple input variables. In such cases the multiple regression model can be described in a matrix format as:

Y = Xb +ε, where,

$$Y = \begin{vmatrix} y_1 \\ y_2 \\ \vdots \\ y_n \end{vmatrix}, \quad X = \begin{vmatrix} 1\, x_{11}\, x_{12} \ldots x_{1p} \\ 1\, x_{21}\, x_{22} \cdots x_{2p} \\ \vdots\ \vdots\ \vdots\ \vdots\ \vdots \\ 1\, x_{n1}\, x_{n2} \cdots x_{np} \end{vmatrix}, \quad b = \begin{vmatrix} b_0 \\ b_1 \\ \vdots \\ b_p \end{vmatrix} \text{ and } \varepsilon = \begin{vmatrix} \varepsilon_1 \\ \varepsilon_2 \\ \vdots \\ \varepsilon_n \end{vmatrix} \quad (17)$$

Simulating Eq. (17) generates multi-dimensional response surfaces (a two dimensional RSM shown in Fig. 4) that can be used to optimize the system based on multiple response variables.

3. Applied methodology and results

For this study, we reviewed literature and selected 115 papers publishing data on QD sensitized solar cells and 65 papers published for ASSSCs to be reviewed and analyzed. This data from a total of 180 independently performed experiments was entered in an excel spreadsheet and the sequence of operation was performed as presented in the flow chart of Fig. 5. The data was checked for completeness in the sense that information, about all the input and output variables that we wanted to include in the analysis, was available or not. Once the data was entered in the spreadsheet, the outliers in the dataset were excluded from the analysis. This screening operation left us with a sample size of 94 experimental data sets for the liquid electrolyte solar cells [18–112] and a sample size of 46 experimental data sets for the ASSSC [113–153].

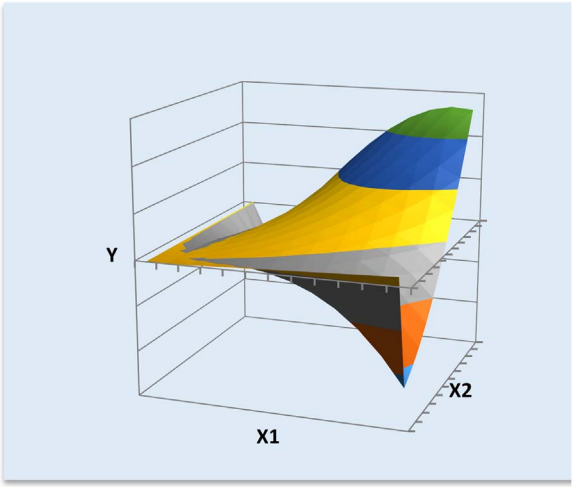

Fig. 4. Arbitrary response surface for the output variable y, that is dependent on two input (independent) variables x_1 and x_2.

The above-mentioned data gathered from the literature was analyzed using commercially available software "DOE Pro 2010". This software is an Excel add-on making it very user friendly, providing an added feature for analyzing historically collected data to detect correlation patterns between inputs and outputs. This software also allows to perform analyses based on attribute or continuous data.

Arbitrary coded numeric values were assigned to various materials (attribute variables) used in the solar cells as given in Tables 1 and 2 to be used by the DOE Pro software as attribute data for correlation analysis. Although arbitrary numeric values were used for all the input variables, the actual values of efficiency (η) and fill factor (FF) observed for the cells were used for each case.

Multivariable regression analyses were performed on the coded data using the DOE Pro software, keeping all the main variables in the analysis systemically eliminating interactions and quadratic terms that do not correspond to at least a 90% confidence level in affecting the output property of interest. In the 2nd iteration of regression analyses we focused on the tolerance values, eliminating those variables from analyses that demonstrated a low (< 0.50) tolerance value (indicating high multicollinearity) to generate the results presented in this paper. Normally a minimum tolerance value of 0.5 is recommended [154], though a minimum recommendation as low as 0.20 has also been found [155] while values as low as 0.25 have been used in regression analyses in the literature [156].

3.1. Results and discussion on regression analyses

It is quite common in applied sciences that properties or qualities of interest (output/dependent variables) are defined by several parameters or factors (input/independent variables). Regression analysis is one of the simplest instruments for obtaining a prediction model for the output variables based on input variables. Factorial regression is where, besides individual independent variables, a combination of various levels of variables is used to forecast the output variables. In other words, factorial regression analyses can be used to evaluate the effects of interaction between two or more independent variables in defining or predicting the dependent variable (or property of interest).

Table 3 presents the detailed regression analyses of the liquid electrolyte solar cells' data for the efficiency of solar cells as well as fill factor observed. The regression coefficient (R^2) for the efficiency of the solar cells is 0.6952, giving an R-value of 0.834 indicating that 83.4% of the variability observed in the efficiency of the solar cells can be explained based on the variables included in the regression analyses.

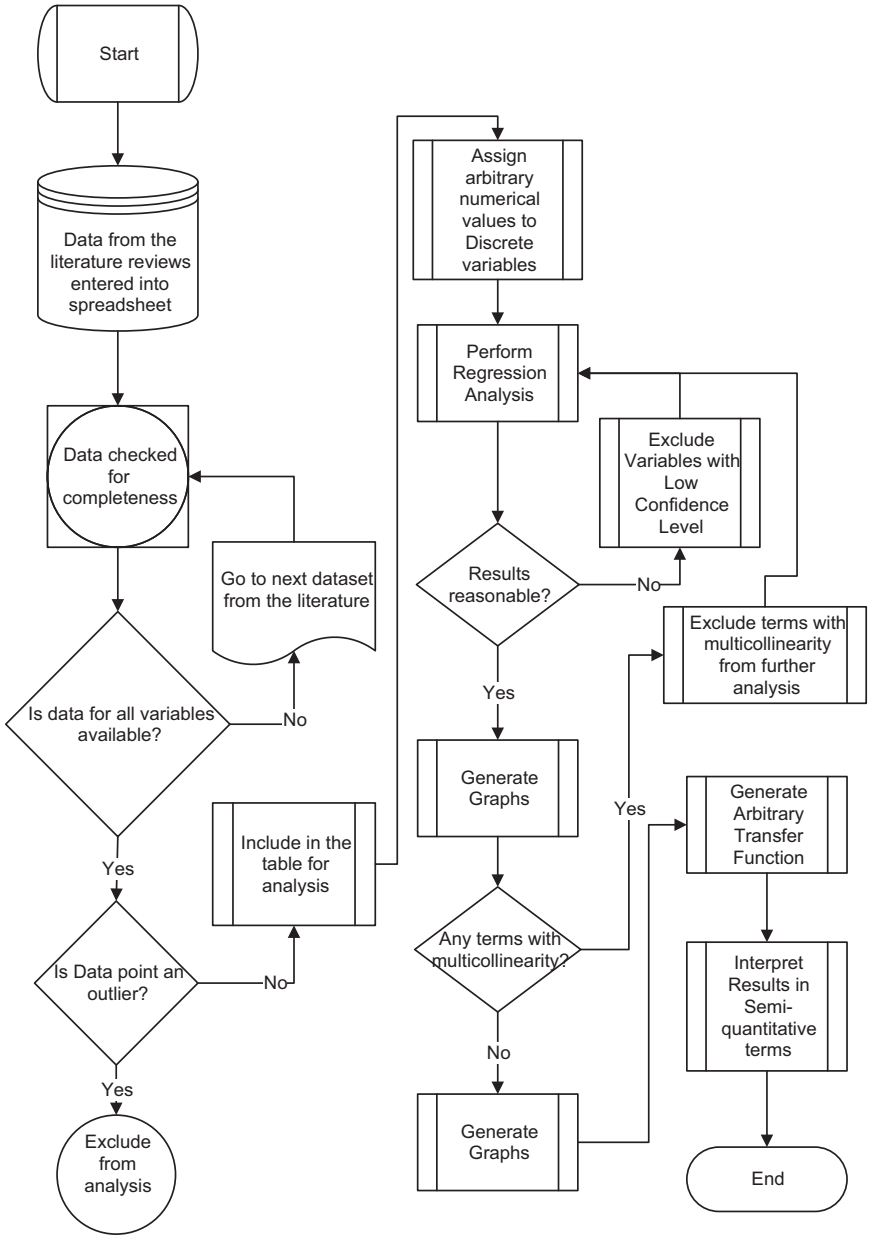

Fig. 5. Process flow diagram for the methodology we applied to the reviewed data to extract useful information for the advancement of improved efficiency and fill factor goals.

The R^2 value for the fill factor on the other hand is low (0.3627) giving a correlation factor R=0.6023 indicating that about 60% of the variation observed in the fill factor can be explained based on the variables selected in the model. The R^2 value may be small, still the p-values obtained from a two-tail *t*-test are indicative that the contributions of individual or a combination of variables tested may be statistically significant [157] in defining the fill factor.

Except for the input variables "electrolyte" and "WBGS", p-value for

Table 1
Arbitrary numeric codes were assigned to different materials as given in the following table for QD sensitized liquid electrolyte solar cells data.

Sensitizer		WBGS		Electrolyte		Counter Electrode		Deposition Method	
Material	**Code**	**Material**	**Code**	**Material**	**Code**	**Material**	**Code**	**Method**	**Code**
CdS, ZnSe	1	Graphene	1	Organic Redox	1	PEDOT	1	Linker	1
CdS	2	ZnO	2	Fe-Based	2	Pt	2	Linker+DA	2
CdSe	3	TiO_2+Graphene	3	Li- Based	3	Au	3	SPD	3
CdTe	4	ZnO+CNT	4	Poly-sulfide	4	Carbon	4	Electrophoretic	4
CdSe+CdTe	5	TiO_2+ZnO	5	P3HT	5	PbS	5	DA	5
CdHgTe+CdTe	6	TiO_2	6	Sulfur/ Sn Based	6	Carbon+Cu_2S	6	CBD	6
CdS+CdSe	7	CNT	7	Na_2S Based	7	CoS	7	SILAR	7
CdSeS+CdSe	8			Co Based	8	Cu_2S	8	Linker+CBD	8
CdSe+Z907Na	9					Cu2S+RGO	9	SILAR+CBD	9

Table 2
Arbitrary numeric codes were assigned to different materials as given in the following table for all solid state QD/perovskite sensitized solar cells data.

Sensitizer		WBGS		Hole Conductor		Counter Electrode	
Material	**Code**	**Material**	**Code**	**Material**	**Code**	**Material**	**Code**
CdS	1	ZnO	1	None	0	Ag	1
CdSe	2	ZnO+TiO_2	2	Spiro-OMeTAD	1	Au	2
CdTe	3	TiO_2	3	P3HT	2	FTO	3
CdS, CdSe	4	Al_2O_3	4	QT12PTA	3	Pt+C60	4
PbS	5	ZrO_2	5	PCBM, P3HT	4		
PbS+PbSe	6			PNV, MoO_x	5		
Sb_2S_3	7			MoO_x	6		
$CH_3NH_3PbBr_3$	8			EDT/MPA	7		
$CH_3NH_3PbI_3$	9			CuSCN	8		
$CH_3NH_3PbI_{1-x}Br_x$	10			PCBTDPP	9		
$CH_3NH_3PbI_2Cl$	11			PCPDTBT	10		
$CH_3NH_3PbI_{3-x}Cl_x$	12			PTAA	11		

all the rest of the variables is less than the generally accepted critical value of $p < 0.05$ indicating that the confidence level is above 95% for the hypothesis that all these variables control the efficiency (Table 3). The p-value for WBGS is 0.0659 which is in the marginal range indicating that the confidence level that the choice of WBGS contributes to the efficiency of a solar cell is only 93.41%. The electrolyte on the other hand has a very high p-value (0.6533) indicating a very low confidence that electrolyte contributes to efficiency of the solar cells. This may simply mean that given the dataset the noise level is so high that it is not possible to quantify the relative effect of the electrolyte on solar cell efficiency. The signal to noise ratio could be improved by collecting data through controlled systematic variation of electrolyte in a statistically designed experimental set-up. Fig. 6 shows Pareto charts for coefficients of regression quantifying the relative contribution of each variable to the efficiency of the solar cells. This shows that the biggest contributors to the efficiency of a solar cell are the "counter electrode" and its interaction with the "WBGS" followed by the "WBGS", the "sensitizer" and the "QD deposition method" with negligible contribution from electrolyte.

Considering the p-values for fill factor in Table 3, all the variables and the interactions are statistically significant at confidence level of

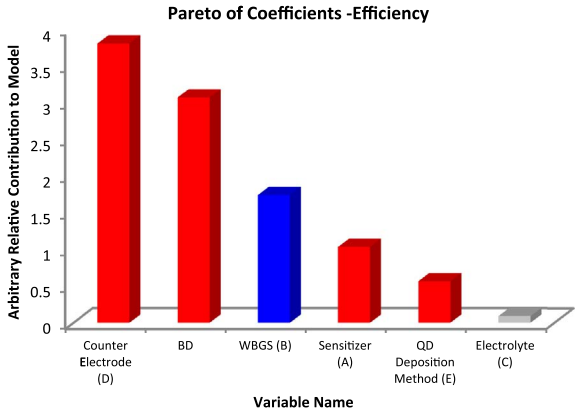

Fig. 6. Pareto of coefficients for all the important factors that affect the efficiency of the liquid electrolyte solar cells. The factors represented by red bars are the ones with confidence level above 95% while the factors with blue bars fall in the marginal confidence level between 90% and 95%. The factors represented by grey bars are not statistically significant and may minimally affect the efficiency. (For interpretation of the references to color in this figure legend, the reader is referred to the web version of this article.)

Table 3
Preliminary Prediction Model for Efficiency η (%) & Fill Factor for reviewed data from Ref#6.

		Efficiency			Fill Factor		
Input variables	**Variable name**	**Regression Coefficient**	**P (2 Tail)**	**Tolerance**	**Regression Coefficient**	**P (2 Tail)**	**Tolerance**
Constant		4.470	0.0000		45.285	0.0000	
A	Sensitizer	1.031	0.0000	0.7862	6.314	0.0115	0.5943
B	WBGS	−1.740	0.0659	0.0233	9.780	0.0000	0.8919
C	Electrolyte	0.09091	0.6433	0.7075	−14.272	0.0000	0.4889
D	Counter Electrode	3.806	0.0056	0.0099	4.226	0.0360	0.8267
E	QD Deposition Method	0.56574	0.0001	0.8031	−3.724	0.1472	0.4592
AE	Sensitizer*QD Dep. Method				−8.169	0.0810	0.4842
BD	WBGS*Counter Electrode	−3.071	0.0241	0.0085			
CC	(Electrolyte)^2				14.862	0.0420	0.5370
	R^2	0.6952			0.3627		
	Adjusted R^2	0.6742			0.3108		
	Standard Error	0.7462			10.1193		
	F	33.0729			6.9906		
	Sig F	0.0000			0.0000		
	F_{LOF}	1.4089			1.0915		
	Sig F_{LOF}	0.1497			0.4022		
	Source	**SS**	**df**	**MS**	**SS**	**df**	**MS**
	Regression	110.5	6	18.4	5010.9	7	715.8
	Error	48.4	87	0.6	8806.5	86	102.4
	$Error_{Pure}$	14.2	32	0.4	3098.9	32	96.8
	$Error_{LOF}$	34.3	55	0.6	5707.6	54	105.7
	Total	158.9	93		13817.4	93	

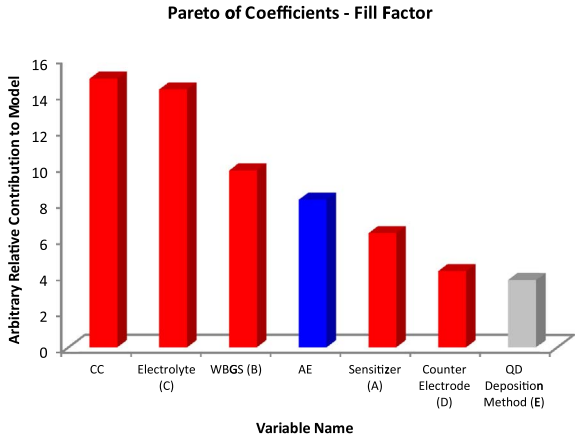

Fig. 7. Pareto of coefficients for all the important factors that affect the fill factor of the liquid electrolyte solar cells. The factors represented by red bars are the ones with confidence level above 95% while the factors with blue bars fall in the marginal confidence level between 90% and 95%. The factors represented by grey bars are not statistically significant and may only minimally affect the fill factor. (For interpretation of the references to color in this figure legend, the reader is referred to the web version of this article.)

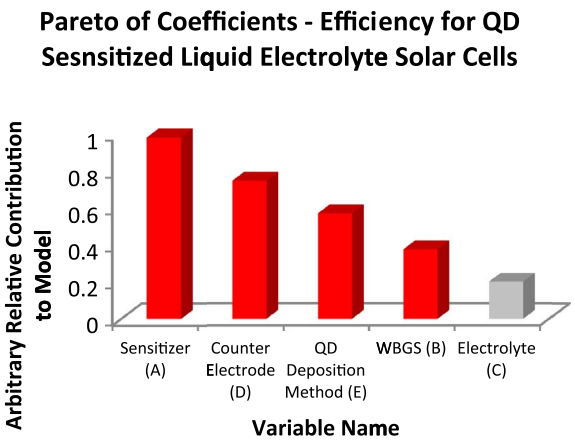

Fig. 8. Pareto of coefficients for all the important factors that affect the efficiency of the liquid electrolyte solar cells after removing the multicollinearity. The factors represented by red bars are the ones with confidence level above 95% while the factors represented by grey bars are not statistically significant and may only minimally affect the efficiency. (For interpretation of the references to color in this figure legend, the reader is referred to the web version of this article.)

above 95% except the interaction of sensitizer with the QD deposition method that is at marginal confidence level of 91.9% and the QD deposition method which is not significant. Fig. 7 shows the Pareto chart of relative quantitative effects of the various factors in determining the FF. The biggest contributors to FF are quadratic and linear contributions of electrolyte, followed by the WBGS, sensitizer's interaction with QD deposition method, sensitizer itself and the counter electrode.

Multicollinearity in Regression Models is an unacceptably high level of intercorrelation among the independent variables, such that the effects of the independent variables cannot be separated. Under multicollinearity, estimates are unbiased but assessments of the relative strength of the explanatory variables and their joint effect are unreliable. Tolerance values in regression analyses are indicative of the extent of multicollinearity, and if the tolerance values observed for a given variable are less than some cut-off value, which we decided to keep at 0.5, the variable should be dropped from the analysis due to multicollinearity [158]. Another set of regression analyses was performed after removing the interaction terms with high multicollinearity (or tolerance values < 0.5) and the results of this exercise are presented in Table 4. The tolerance values and the p-values of the remaining terms in the model have improved providing us higher confidence in the results.

Figs. 8 and 9 show the Pareto of regression coefficients for efficiency of the solar cell and the FF respectively. There is significant difference between what we observed in Figs. 6 and 7 and what is observed here. The results presented in Figs. 6 and 7 only represented the qualitative importance of various factors while Figs. 8 and 9 show quantitative relative importance of each statistically significant factor in order of their importance in determining the efficiency and FF of the QD sensitized solar cells. Fig. 8 shows that for improving the efficiency of a solar cell, choice of an appropriate sensitizer has the biggest impact, followed by the counter electrode material, then QD deposition method and finally the least important factor is the WBGS material. The electrolyte plays minimal role (statistically non-significant or SNS) in determining the efficiency of a solar cell in relation to other variables considered here.

On the other hand, electrolyte and its quadratic term are two most important factors for improving the fill factor. These are followed by

Table 4
Prediction Model for Efficiency η (%) and Fill Factor for reviewed data from Ref#6 after removal of interaction factors with multicollinearity.

		Efficiency			Fill Factor		
Input Variables	**Variable Name**	**Regression Coefficient**	**P (2 Tail)**	**Tolerance**	**Regression Coefficient**	**P (2 Tail)**	**Tolerance**
Constant		2.297	0.0000		45.502	0.0000	
A	Sensitizer	0.98267	0.0000	0.8006	4.140	0.0562	0.7960
B	WBGS	0.37698	0.0156	0.9119	9.363	0.0000	0.9040
C	Electrolyte	0.20157	0.3020	0.7532	−13.931	0.0000	0.4907
D	Counter Electrode	0.74911	0.0000	0.8337	4.038	0.0471	0.8291
E	QD Deposition Method	0.57148	0.0002	0.8033	−0.78596	0.6879	0.8016
CC	$(\text{Electrolyte})^2$				11.647	0.1022	0.5737
	R^2	0.6767			0.3395		
	Adjusted R^2	0.6584			0.2940		
	Standard Error	0.7640			10.2418		
	F	36.8455			7.4546		
	Sig F	0.0000			0.0000		
	F_{LOF}	1.5021			1.1316		
	Sig F_{LOF}	0.1084			0.3592		
	Source	**SS**	**df**	**MS**	**SS**	**df**	**MS**
	Regression	107.5	5	21.5	4691.6	6	781.9
	Error	51.4	88	0.6	9125.7	87	104.9
	$Error_{Pure}$	14.2	32	0.4	3098.9	32	96.8
	$Error_{LOF}$	37.2	56	0.7	6026.9	55	109.6
	Total	158.9	93		13817.4	93	

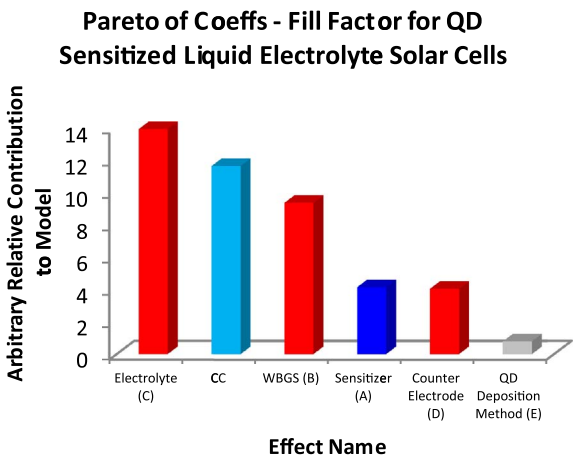

Fig. 9. Pareto of coefficients for all the important factors that affect the fill factor of the liquid electrolyte solar cells. The factors represented by red bars are the ones with confidence level above 95%, the factors with blue bars fall in the confidence level below 95% but above 90%, and the factor represented by light blue bars are with confidence level between 80% and 90%. The factors represented by grey bars are not statistically significant and may only minimally affect the fill factor. (For interpretation of the references to color in this figure legend, the reader is referred to the web version of this article.)

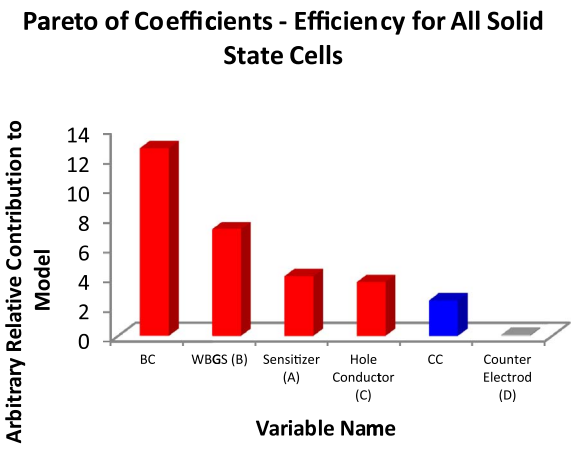

Fig. 10. Pareto of coefficients for all the important factors that affect the efficiency of the all solid state solar cells. The factors represented by red bars are the ones with confidence level above 95% while the factors with blue bars fall in the marginal confidence level between 90% and 95%. The factors represented by grey bars are not statistically significant and may only minimally affect the efficiency. (For interpretation of the references to color in this figure legend, the reader is referred to the web version of this article.)

WBGS material, then sensitizer material and the counter electrode plays the least important role while QD deposition method plays minimal or statistically non-significant role in affecting the value of the FF in a solar cell (Fig. 9). The regression coefficients obtained in Table 4 can be used to define a pseudo-transfer function as given in the following equations:

$$\eta \approx 2.3 + 0.98 \times S + 0.38 \times W + 0.75 \times C_E + 0.57 \times Q_D \quad (18)$$

$$FF \approx 45.5 + 4.14 \times S + 9.36 \times W + 4.04 \times C_E + 11.65 \times E_L^2 - 13.93 \times E_L \quad (19)$$

Here S = Sensitizer, W = WBGS, C_E = Counter Electrode, Q_D = QD Deposition Method, and E_L = Electrolyte.

We term the Eqs. (18) and (19) as pseudo-transfer functions in the sense that the factors used are attribute factors and do not have real numerical values and are only assigned numeric values to extract the vital information needed to set the direction of research for improving both the efficiency as well as the fill factor in solar cells. Eq. (18) demonstrates that even though every factor has different relative importance all the factors play a supporting role in improving the efficiency of the solar cells. On the other hand, Eq. (19) shows that the electrolyte plays both a positive as well as a negative role in determining the FF for the solar cells. In its negative role, it is opposing the effects of sensitizer, WBGS and counter electrode.

Table 5 represents the regression analyses for all solid state solar cells (ASSSC) data reviewed before and after removing the interaction factors with high multicollinearity (Tolerance < 0.5). Figs. 10 and 11 show the corresponding Pareto charts for variables that impact the efficiency of the ASSSC. Table 5 and Fig. 10 demonstrate that although the interaction between hole conductor and WBGS, WBGS itself, the sensitizer and the hole conductor are statistically significant, because of the high multicollinearity of the interaction term, it is not possible to evaluate the quantitative relative importance of each factor indepen-

Table 5
Prediction Model for Efficiency η (%) for reviewed data from Ref#12 for all solid state solar cells, before and after the removal of interaction factors with multicollinearity.

		Prediction Model based on p-value			Prediction Model based on p-value and Removed Multicollinearity		
Input Variables	**Variable Name**	**Regression Coefficient**	**P (2 Tail)**	**Tolerance**	**Regression Coefficient**	**P (2 Tail)**	**Tolerance**
Constant		1.610	0.2008		4.616	0.0000	
A	Sensitizer	4.032	0.0000	0.6724	4.374	0.0000	0.6844
B	WBGS	−7.211	0.0109	0.2135	0.46453	0.7664	0.8055
C	Hole Conductor (HC)	−3.623	0.0124	0.1586	0.44444	0.5370	0.7434
D	Counter Electrode	0.07393	0.9460	0.9210	0.13382	0.9127	0.9212
BC	WBGS*HC	−12.683	0.0020	0.1185			
CC	$(HC)^2$	2.390	0.0771	0.7398	1.917	0.1978	0.7486
R^2		0.6449			0.5447		
Adjusted R^2		0.5903			0.4878		
Standard Error		2.2992			2.5709		
F		11.8072			9.5703		
Sig F		0.0000			0.0000		
F_{LOF}		1.0760			1.4516		
Sig F_{LOF}		0.4668			0.2520		
Source		**SS**	**df**	**MS**	**SS**	**df**	**MS**
Regression		374.5	6	62.4	316.3	5	63.3
Error		206.2	39	5.3	264.4	40	6.6
$Error_{Pure}$		60.3	12	5.0	60.3	12	5.0
$Error_{LOF}$		145.9	27	5.4	204.1	28	7.3
Total		580.7	45		580.7	45	

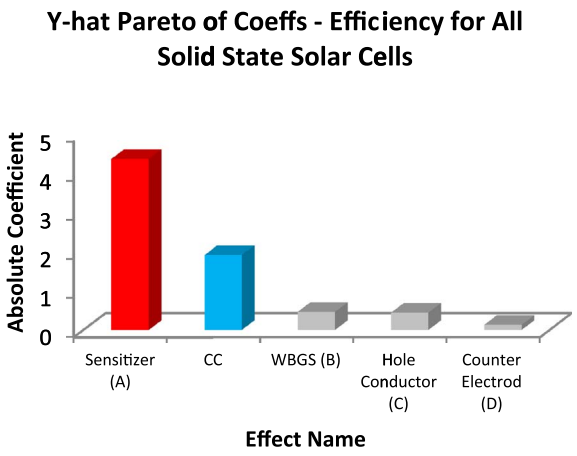

Fig. 11. Pareto of coefficients for all the important factors that affect the efficiency of the all solid state solar cells after removing the multicollinearity. The factors represented by red bars are the ones with confidence level above 95% and the factor represented by light blue bar is with confidence level between 80% and 90%. The factors represented by grey bars are not statistically significant and may only minimally affect the efficiency. (For interpretation of the references to color in this figure legend, the reader is referred to the web version of this article.)

dently. Last three columns in Table 5 and Fig. 11 show the true relative importance of the factors that are statistically significant and whose effects can be evaluated independent from each other.

Fig. 11 shows that like liquid electrolyte solar cells; the choice of the sensitizer material is the most important factor that controls the efficiency of ASSSC. From Table 5 we also see that we are just more than 80% confident that the choice of hole conductor material quadratically effects the efficiency of the ASSSC. The regression coefficients obtained from Table 5 can be used to develop a pseudo transfer function for the efficiency of ASSSC like Eqs. (18) and (19). The pseudo transfer function for ASSSC is thus given as:

$$\eta \approx 4.62 + 4.37 \times S + 1.92 \times H_C^2 \quad (20)$$

where S=Sensitizer and H_C=Hole Conductor.

3.2. Discussion on sensitizers – the most important factor

The Pareto of coefficients presented in Figs. 8 and 11 represent the factors affecting the efficiency of liquid electrolyte based solar cells and ASSSC respectively. In both cases the factor having the highest impact on the efficiency is the QD sensitizer, indicating that if one was to focus on only one factor to improve the efficiency of the solar cells, it ought to be the sensitizer. This analysis for efficiency was repeated with another set of literature data containing 19 independent experiments [159–172]. In this data, the combination of variables and constants was different, thus could not be combined with the earlier data. However, this analysis confirmed sensitizer to be the most important factor for defining efficiency of quantum dot sensitized solar cells. The idea of using quantum dots for charge pumping is based on conversion of optical excitation into deterministic electric current [173]. Sensitizer is thus the heart of the sensitized solar cells as this is where incident photons interact with the charge carriers that eventually produce the photocurrent.

The defining property of a semiconductor is that there is an energy gap (bandgap) between filled electron energy states (valence band) and allowed discrete mostly empty energy states (conduction band). A QD used as sensitizer is a small semiconductor box and the bandgap between the valence band and the conduction band increases (generally known as blue shift) as the QD size gets smaller if the Coulomb interactions remain ineffective. However, the shift in bandgap to lower energy (a red shift) is observed when the QD size becomes too small such that Coulomb interactions become the dominating ones [174]. Thus, quantum confinement is the dominant contribution as the radius of the dot is reduced, until the stage is reached when Coulomb interactions become more important that can lead to a red shift in the absorption spectrum. This is where the unfavorable consequence of the spatial confinement of electrons and holes in QDs becomes dominant and the probability of recombination of an electron in the conduction band and a hole in the valence band increases.

There are plenty of atoms and electrons in the region of the QD but most of them lie in the valence band and require energy of the order of 1 eV to be excited. When these semiconductor QDs are irradiated with light, the absorption of light takes place and consequently transitions from the valance band into conduction band occur if the energy of incident photons is equal to or greater than the bandgap. There is a minimum energy at which absorption can take place. Light with lower energy cannot be absorbed, no matter how intense. On the other hand, light with energy higher than bandgap energies can be absorbed resulting in electrons making the transition into higher energy states; there are also more tightly bound valence states (deep states) that could be excited. Thus, QDs show truly discrete excitation spectra that are like those of natural atoms. The energy of the absorbed photon that is more than the bandgap energy is transferred to the excited electron-hole pair as their kinetic energy thus creating “hot electrons” and “hot holes”.

Electron phonon interactions play key roles in the applications of QDs in solar cells and carry significant fundamental and practical importance [175]. The excess energy of hot electrons and hole can be wasted as heat through electron-phonon scattering and subsequently phonon emission [176]. The decay of the highly-excited electrons in QDs through coupling with phonons results in voltage and current losses, and therefore, it should be avoided [177]. However, the excess energy of hot electron-hole pair can be used to improve the efficiency of the solar cells by (a) immediate extraction from the QD (photoelectron collection) before they cool to band edges – this improves the photo-voltage [178,179] or (b) production of additional electron hole pairs through impact ionization – this will produce enhanced photocurrent [180,181].

The nanostructuring of the semiconductor materials into QDs for solar cell applications introduces profound changes in its properties. Some researchers declare that a depletion layer (like that observed in conventional solar cells) cannot be formed in the QD solid — the particles are simply too small [182]. Thus, there is no significant local electric field present to assist in the separation of photo-generated electron-hole pairs. Blanton et al. [183] and Schmidt et al. [184] on the other hand measured a potential drop of 0.25 V across the dot for CdSe QDs with diameters of 3.4 and 4.6 nm and considered this to be intrinsic to the wurtzite structure. Tomasulo and Ramakrishna [185] suggested that reasonably reliable results can be obtained for exciton energies by using the local ‘empirical’ pseudopotential method, except in the case of the smallest QDs, when it is more appropriate to include non-local corrections. Recently, intentionally n-doped wide bandgap semiconductors such as TiO_2 [186], ZnO [187] and CdS [188] have been deployed to form a junction and hence a depletion region with p-type colloidal QDs with improved charge collection [189,190].

In summary, the most important processes and factors related to the sensitizer that define the efficiency depend on the absorption of incident photons resulting in photoelectron generation and enhanced availability of generated charge carriers for photocurrent in QD based solar cells. There are several phenomena observed in solar cells like photoelectron generation, electron-phonon interaction and relaxation, phonon dephasing, electron trapping, recombination etc. However, all these are driven by some fundamental QD physical properties like, the material type (determines QD bandgap), the QD size (determines the Quantization level of the bandgap), the nanostructure and morphology of the QD, presence of impurities in QD and surface and interface states in the QDs. Although study of all the physical phenomenon help us understand what actions to take to improve the properties of QDs

for specific applications, of functional significance, the parameters to consider, from applications point of view, are the choice of material, the size of the QD, the nanostructure (including QD surface structure) and doping level of the QD to control the entire physics of the QDs. What process parameters can control these physical properties of QDs during the synthesis for the desired application are of practical significance and will in turn depend on the technique used for fabrication of QDs.

3.3. Extraction of charge carriers and photocurrent generation

A sensitizer in a solar cell is where the charge carriers are generated. The next stage in the functioning of solar cell is the extraction of the generated photoelectrons to produce a photo-voltage and photocurrent. There are several factors that can control this process. For example, the electrons generated must leave the QD and travel through the WBGS and then are collected at the electrode made from a transparent conducting material. While on the other hand holes' travel through the electrolyte and are collected at the counter-electrode. The types of materials used in each of these factors determine the exact mechanism and efficiency of this transfer of electrons and holes to their respective electrodes for collection. In Fig. 8, we observed that for the liquid electrolyte based QD sensitized solar cells, after the sensitizer, the most important factor controlling the efficiency of the solar cells is the counter-electrode used. While for the ASSSCs, where a hole conductor replaces the liquid electrolyte the most important factor after the sensitizer is the hole conductor (Fig. 11) and this has a quadratic effect in defining the efficiency of the solar cell.

Fig. 12(a) shows the schematic of electron and hole paths in a QD sensitized liquid electrolyte solar cell. The photoelectrons generated in the QD are transferred to the WBGS through which they travel to the transparent conducting electrode material where they become available for electricity production. The holes on the other hand are transferred through a Redox reaction to electrolyte where ions are freely mobile and move to the counter-electrode to extract an electron to neutralize the hole transferred from the sensitizer. So, in this type of device, the ease of electron extraction from the counter electrode will dominate the performance of the solar cell, after the sensitizer (Fig. 8).

On the other hand, in an ASSSCs, a hole conductor replaces the liquid electrolyte. As shown in Fig. 12(b), in this case, the electrons from the counter-electrode are transferred through a hopping mechanism within the hole conductor to the sensitizer to neutralize the photo-generated holes. In this case the ease of conduction of holes through the hole conductor will dominate the performance of the final solar cell device, after the sensitizer (Fig. 11).

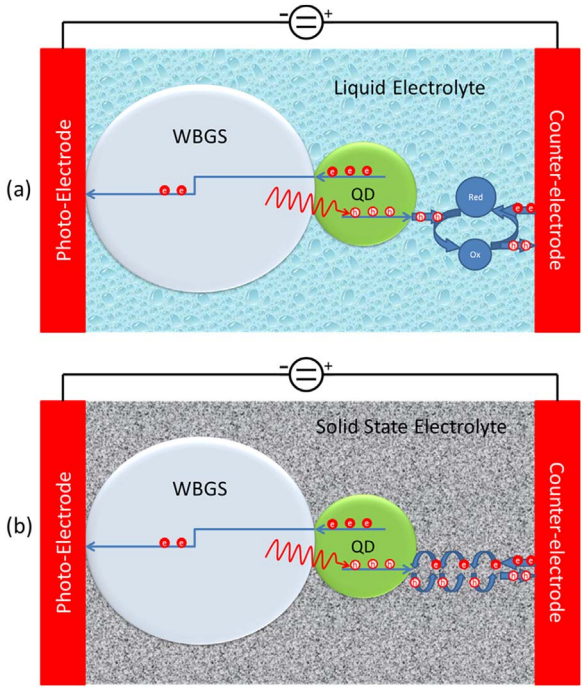

Fig. 12. Models for the electron transfer mechanism and generation of photocurrent in (a) liquid electrolyte solar cells (b) all solid state solar cells.

Due to limited availability of data for our analysis on ASSSCs, there is nothing further we can say about ASSSCs besides that sensitizer and the hole conductor are the two most important factors that determine the efficiency of these solar cells. The impact of everything else is buried in the noise and more controlled experimental data is required to quantify those impacts. However, in case of liquid electrolyte solar cells, after the sensitizer and the counter-electrode the next most important factor that controls the efficiency of these solar cells is the QD deposition method (Fig. 8). This is quite conceivable as to achieve higher efficiency for solar cells, the rates of photo-generated electron transport and interfacial transfer across the contacts to the electrode must be fast compared to the rate of carrier cooling [175,191,192]. And it is the QD deposition method that will determine the state of interface between the QD and the WBGS and how easy it is for an electron to cross this interface. Exploitation of the interaction between inorganic quantum dots and organic, inorganic, or hybrid ligand and cross-linker systems has played a central role in performance improvements [193–198]. The ligand exchange process has also been tuned to optimize inter-quantum-dot spacing, enhancing charge-carrier mobility [199–201].

Once the photo-generated electrons cross the interface and enter the WBGS, their mobility within the WBGS material would start to dominate and that is why we find that the next factor in order of importance for the efficiency, in our analysis presented in Fig. 8 is the WBGS. However, only a handful of WBGS materials had been exploited so far and among all those tried, TiO_2 has found the greatest attraction. Some authors [202–204] performed comparative studies on the electrical characteristics of the TiO_2, ZnO and SnO_2 as WBGS in solar cells and found TiO_2 to be the best performing WBGS so far among these three, presumably the main reason for opting to use this WBGS in solar cells.

3.4. Fill factor – the cell quality parameter

The fill factor (FF) is a parameter often used to describe the quality of a solar cell and is defined as:

$$FF = \frac{V_{max} \times I_{max}}{V_{oc} \times I_{sc}} \quad (21)$$

Eq. (21) shows that to improve the FF, one must improve the maximum voltage (V_{max}) and the maximum current (I_{max}). In QD solar cells, under light illumination, a voltage is generated, corresponding to the difference of the Fermi level of the electron in the metal oxide and the redox potential of the electrolyte [205–207]. For a given metal oxide used as the WBGS material the electrolyte plays the most vital role in determining the fill factor as is evident from Fig. 9 and Eq. (19). As has been discussed already, the electrolyte plays a dual role in defining the FF, a positive one and a negative one. In its positive role, it is supporting the effects of sensitizer, WBGS and counter electrode, while in its negative role it opposes these effects.

We present a model to explain these two roles in Fig. 13 with process B and A respectively. Let's assume that 2 electron-hole pairs are generated in each of the QD1 and QD2 because of photo-absorption. Ideally, all the four electrons should be collected at the photo-electrode and the holes should be collected at the counter-electrode giving rise to a 100% collection efficiency. However, as shown in process A, the two holes generated in QD1 can recombine with the two electrons generated in QD2 through a redox reaction, resulting in only a transfer of two electrons to the photo-electrode and two holes to counter-electrode. This reduces the collection efficiency to 50% that

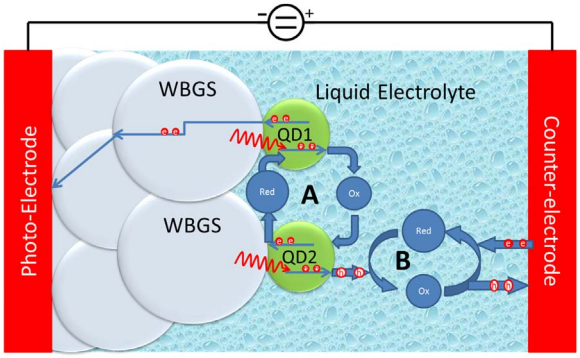

Fig. 13. A simple model for the positive as well as negative roles of a liquid electrolyte in solar cells. The process 'A' plays a negative role, reducing the collection efficiency, while the process 'B' plays a supporting role in generating the photocurrent.

leads to a reduction in the photocurrent and consequently the FF.

The next two most important parameters for fill factor are WBGS material and the sensitizer material that make up the photo-electrode (Fig. 9). It has already been suggested by Mora-Seroì et al. [208] and Guijarro et al. [209] that besides the recombination processes at the electrode/electrolyte interface, the electron injection from QD to WBGS play a very important role in governing the photo-conversion. Finally, a suitable choice of the counter electrode also contributes to the FF positively.

To improve the FF and eventually the overall efficiency of the solar cell, the process like "A" in Fig. 13 need to be suppressed and ways and means need to be discovered to improve on processes like "B". FF can be improved by improving on photo-voltage as well as photocurrent. Photo-voltage increases because of hydrogenation of TiO_2 films [209], doping of TiO_2 with Nb [210], improving the charge transport properties of a redox couple in the electrolyte and reducing the recombination at the interface between QD-TiO_2 photo-electrode and the electrolyte [211]. The increase in photocurrent arises from both an increase in the absorption in the quantum dots and a decrease in the carrier recombination [212]. It has already been discussed that to improve on the photo-voltage the hot-carriers generated in the QD are to be collected before they cool, and to improve on photocurrent, processes for multiple electron generation because of impact ionization need to be strengthened.

3.5. Optimization of efficiency and fill factor

Table 6 presents the percent contribution from each of the individual key component of the solar cell, i.e. QD Sensitizer, WBGS, electrolyte or in case of ASSSCs the hole conductor, counter electrode and the QD deposition method, to the efficiency and the fill factor of the final device. From this table, we can see that sensitizer and WBGS combined (that make the active or photo-electrode) explain 51% variation and adding the QD deposition method to the mix covers 72% of the variation observed in the efficiency of the liquid electrolyte solar cells. On the other hand, electrolyte alone covers almost 60% of the variation observed in the fill factor in the literature, adding the above mix to it we can explain almost 90% of the variation in the fill factor. In case of the ASSSCs, sensitizer alone can explain almost 60% of the variation in the efficiency, another almost 32% of the variation can be explained by the hole conductor, combined cover 91.35% of variation observed in the efficiency of the ASSSCs from the literature.

Table 6
Percent contribution of various factors studied in the literature to the efficiency and fill factor.

	% Contribution in Liquid Electrolyte Solar Cells		% Contribution in ASSSC
Factor	**Efficiency**	**Fill Factor**	**Efficiency**
Sensitizer	37%	9.5%	59.5%
Counter Electrode	28%	9.3%	1.89% but SNS
QD Deposition Method	21%	Negligible and SNS	No data included
WBGS	14%	21.8%	6.76% and SNS
Electrolyte	Negligible and SNS	59.4%	31.89%

As described earlier, response surface methodology (RSM) consists of a group of mathematical and statistical techniques used in the development of an adequate functional relationship between a response of interest (or output variables), efficiency (η) and FF in the case of solar cells, and several associated controls (or input) variables [213]. The best parameter setting for the input variables can be determined by using the RSM to optimize multiple response variables. The response surface of a concerned response is selected as the objective function, and the remaining response surfaces are selected as constraint functions. Mathematical/computer programming is then utilized to acquire the solution to the optimization problem [214]. We used RSM to find out what combination of materials would provide us the best outcome for solar cell efficiency and FF in case of liquid electrolyte and the efficiency in case of ASSSCs.

For the reviewed data, we analyzed here, the maximum experimental efficiency observed has been 5.42%, while the maximum experimental value for FF used was 89%, for the liquid electrolyte solar cells. However, it should also be noted that the cell reporting maximum efficiency of 5.42% only had a FF of 47%, while the cell reporting maximum value 89% for FF had an efficiency of only 3.2%. Our RSM analyses of the reviewed data for liquid electrolyte based QD sensitized solar cells reveals that within the design space of the literature reviewed above, an efficiency and FF for such solar cells can reach potentially 7% and 76% respective within a single cell with the following combination of materials: TiO_2, used as WBGS, sensitized by CdSe QDs that are co-sensitized with Z907Na dye, deposited with SILAR & CBD, an Organic Redox is used as electrolyte with a counter-electrode made out of Cu_2S and Reduced Graphene Oxide (RGO). A combination of materials that has not been used so far for fabrication of solar cells in the literature.

Similar analyses for the ASSSCs revealed that these have a potential of reaching an efficiency of about 20% if ZrO_2 WBGS is sensitized with $CH_3NH_3PbI_{3-x}Cl_x$ QDs, poly-tri-aryl-amine (PTAA) is used as the hole conductor and a counter-electrode is made from Pt+C60. This is significantly higher (33% higher) than the experimentally reported data that we used in our analysis where the maximum efficiency for ASSSCs was 15%. Obviously, the predicted efficiency is still way lower than theoretically achievable efficiency (85%) for such solar cells [215]. This indicates that the researchers need to think out of the box and develop new materials and combinations thereof to eliminate various charge losses to achieve efficiency that is beyond predicted 20%.

4. Conclusions

In concluding, we have demonstrated that the methodology we have utilized to review the historical (published) data on liquid and all solid state QD solar cells is a very powerful tool for reviewing the literature and transforming independently collected technical information into an alternative point of view on undefined and not well understood relations amongst a multitude of system variables. Application of this methodology has provided us with previously unknown information regarding relative quantitative importance of each variable in defining the efficiency and fill factor in QD sensitized solar cells or Perovskite ASSSCs. We show that regardless of the type of the solar cell (liquid or all solid state) sensitizer plays the most important role in defining the efficiency of solar cell, while the choice of electrolyte plays a dual role, supporting as well as opposing the fill factor, but plays minimal or

statistically non-significant role in controlling the efficiency of the solar cell. The photo-electrode and the method used to prepare it make a 72% contribution to the efficiency of the solar cell. The photo-electrode combined with electrolyte make a 90% contribution to the fill factor. To improve on the efficiency as well as the fill factor of the solar cells the future research should be focusing on the appropriate choice of the photo-electrode and the electrolyte, may be even investigating new materials to be used as the photo-electrode and electrolyte. The RSM is another powerful tool when combined with our methodology to predict the combination best suited for achieving the research goals faster, at the lowest cost and with minimum possible steps.

Appendix A. Supplementary material

Supplementary data associated with this article can be found in the online version at doi:10.1016/j.rser.2017.01.137.

References

[1] Grätzel M, Janssen RAJ, Mitzi DB, Sargent EH. Materials interface engineering for solution – processed photovoltaics. Nature 2012;488:304–12.
[2] Report by Office of Science US Department of Energy on Workshop Entitled "Basic Research Needs for Carbon Capture: Beyond 2020", March 4–5; 2010.
[3] Rühle S, Shalom M, Zaban A. Quantum-dot-sensitized solar cells. ChemPhysChem 2010;11:2290–304.
[4] Liu M, Johnston MB, Snaith HJ. Efficient planar heterojunction perovskite solar cells by vapour deposition. Nature 2013;501:395–8.
[5] Gonzalez-Pedro V, Juarez-Perez EJ, Arsyad W-S, Barea EM, Fabregat-Santiago F, Mora-Sero I, Bisquert J. General working principles of $CH_3NH_3PbX_3$ perovskite solar cells. Nano Lett 2014. http://dx.doi.org/10.1021/nl404252e.
[6] Jun HK, Careem MA, Arof AK. Quantum dot-sensitized solar cells perspective and recent developments: a review of Cd chalcogenide quantum dots as sensitizers. Renew Sustain Energy Rev 2013;22:148–67.
[7] Zhang G, Finefrock S, Liang D, Yadav GG, Yang H, Fang H, Wu Y. Semiconductor nanostructure-based photovoltaic solar cells. Nanoscale 2011;3:2430–43.
[8] Mora-Sero I, Bisquert J. Breakthroughs in the development of semiconductor-sensitized solar cells. J Phys Chem Lett 2010;1:3046–52.
[9] Etgar L. Semiconductor nanocrystals as light harvesters in solar cells. Materials 2013;6:445–59.
[10] Zhao Y, Burda C. Development of plasmonic semiconductor nanomaterials with copper chalcogenides for a future with sustainable energy materials. Energy Environ Sci 2012;5:5564–76.
[11] Hetsch F, Xu X, Wang H, Kevshaw SV, Rogach AL. Semiconductor nanocrystal quantum dots as solar cell components and photosensitizers: materials, charge transfer, and separation aspects of some device technologies. J Phys Chem Lett 2011;2:1879–87.
[12] Rhee JH, Chung C-C, Diau EW-G. A perspective of mesoscopic solar cells based on metal chalcogenide quantum dots and organometal-halide perovskites. NPG Asia Mater 2013;5:e68. http://dx.doi.org/10.1038/am.2013.53.
[13] Maathuis MH, Colombo D, Kalisch M, Bühlmann P. Predicting causal effects in large-scale systems from observational data. Nat Methods 2010;7(4):247–8.
[14] Waltz D, Buchanan BG. Automating science. Science 2009;374:43–4.
[15] Blow N. High-throughput screening: designer screens. Nat Methods 2009;6(1):105.
[16] Tseng CG, Ghosh D, Feingold E. Comprehensive literature review and statistical considerations for microarray meta-analysis. Nucleic Acids Res 2012;40(9):3785–99.
[17] Nieuwenhuys A, Papageorgiou E, Pataky T, De Laet T, Molenaers G, Desloovere K. Literature review and comparison of two statistical methods to evaluate the effect of botulinum toxin treatment on gait in children with cerebral palsy. PLoS One 2016;11(3):e0152697. http://dx.doi.org/10.1371/journal.pone.0152697.
[18] Kongkanand A, Tvrdy K, Takechi K, Kuno M, Kamat PV. Quantum dot solar cells. tuning photoresponse through size and shape control of CdSe–TiO_2 architectureJ. J. Am Chem Soc 2008;130:4007–15.
[19] Salant A, Shalom M, Hod I, Faust A, Zaban A, Banin U. Quantum dot sensitized solar cells with improved efficiency prepared using electrophoretic deposition. ACS Nano 2010;4:5962–8.
[20] Salant A, Shalom M, Tachan Z, Buhbut S, Zaban A, Banin U. Quantum rod-sensitized solar cell: nanocrystal shape effect on the photovoltaic properties. Nano Lett 2012;12:2095–100.
[21] Fang B, Kim M, Fan S-Q, Kim JH, Wilkinson DP, Ko J, Yu J-S. Facile synthesis of open mesoporous carbon nanofibers with tailored nanostructure as a highly efficient counter electrode in CdSe quantum-dot-sensitized solar cells. J Mater Chem 2011;21:8742–8.
[22] Luan C, Vaneski A, Susha AS, Xu X, Wang H-E, Chen X, Xu J, Zhang W, Lee C-S, Rogach AL, Zapien JA. Facile solution growth of vertically aligned ZnO nanorods sensitized with aqueous CdS and CdSe quantum dots for photovoltaic applications. Nano Res Lett 2011;6:340 ⟨http://nanoscalereslett.springeropen.com/articles/10.1186/1556-276X-6-340⟩.
[23] Chang C-H, Lee Y-L. Chemical bath deposition of CdS quantum dots onto mesoscopic TiO_2 films for application in quantum-dot-sensitized solar cells. Appl Phys Lett 2007;91:053503. http://dx.doi.org/10.1063/1.2768311.
[24] Chou C-Y, Lee C-P, Vittal R, Ho K-C. Efficient quantum dot-sensitized solar cell with polystyrene-modified TiO_2 photoanode and with guanidine thiocyanate in its polysulfide electrolyte. J Power Sources 2011;19:6595–602.
[25] Barea EM, Shalom M, Gimenez S, Hod I, Mora-Sero I, Zaban A, Bisquert J. Design of injection and recombination in quantum dot sensitized solar cells. J Am Chem Soc 2010;132:6834–9.
[26] Zhao F, Tang G, Zhang J, Lin Y. Improved performance of CdSe quantum dot-sensitized TiO_2 thin film by surface treatment with $TiCl_4$. Electrochim Acta 2012;62:396–401.
[27] Chen G, Wang L, Zou Y, Sheng X, Liu H, Pi X, Yang D. CdSe quantum dots sensitized mesoporous TiO_2 solar cells with CuSCN as solid-state electrolyte. J Nanomater 2011;11:40. http://dx.doi.org/10.1155/2011/269591.
[28] Zhu G, Su FF, Lv T, Pan LK, Sun Z. Au nanoparticles as interfacial layer for CdS quantum dot-sensitized solar cells. Nanoscale Res Lett 2010;5:1749. http://dx.doi.org/10.1007/s11671-010-9705-z.
[29] Zhu G, Pan L, Xu T, Sun Z. CdS/CdSe Co-sensitized TiO_2 photoanode for quantum-dot-sensitized solar cells by a microwave-assisted chemical bath deposition method. ACS Appl Mater Interfaces 2011;3:3146–51.
[30] Zhu G, Pan L, Xu T, Sun Z. Microwave assisted chemical bath deposition of CdS on TiO_2 film for quantum dot-sensitized solar cells. J Electroanal Chem 2011;659:205–8.
[31] Zhu G, Pan L, Xu T, Zhao Q, Sun Z. Cascade structure of TiO_2/ZnO/CdS film for quantum dot sensitized solar cells. J Alloy Compd 2011;509:7814–8.
[32] Zhu G, Lv T, Pan L, Sun Z, Sun C. All spray pyrolysis deposited CdS sensitized ZnO films for quantum dot-sensitized solar cells. J Alloy Compd 2011;509:362–5.
[33] Zhu G, Xu T, Lv T, Pan L, Zhao Q, Sun Z. Graphene-incorporated nanocrystalline TiO_2 films for CdS quantum dot-sensitized solar cells. J Electroanal Chem 2011;650:248–51.
[34] Zhu G, Cheng Z, Lv T, Pan L, Zhao Q, Sun Z. Zn-doped nanocrystalline TiO_2 films for CdS quantum dot sensitized solar cells. Nanoscale 2010;2:1229–32.
[35] Lan G-Y, Yang Z, Lin Y-W, Lin Z-H, Liao H-Y, Chang H-T. A simple strategy for improving the energy conversion of multilayered CdTe quantum dot-sensitized solar cells. J Mater Chem 2009;19:2349–55.
[36] Chen H, Fu W, Yang H, Sun P, Zhang Y, Wang L, Zhao W, Zhou X, Zhao H, Jing Q, Qi X, Li Y. Photosensitization of TiO_2 nanorods with CdS quantum dots for photovoltaic devices. Electrochim Acta 2010;56:919–24.
[37] Chen H, Li W, Liu H, Zhu L. CdS quantum dots sensitized single- and multi-layer porous ZnO nanosheets for quantum dots-sensitized solar cells. Electrochem Comm 2011;13:331–4.
[38] Wang H, Luan C, Xu X, Kershaw SV, Rogach AL. In situ versus ex situ assembly of aqueous-based thioacid capped CdSe nanocrystals within mesoporous TiO_2 films for quantum dot sensitized solar cells. J Phys Chem C 2012;116:484–9.
[39] Lee HJ, Chang DW, Park S-M, Zakeeruddin SM, Gratzel M, Nazeeruddin MK. CdSe quantum dot (QD) and molecular dye hybrid sensitizers for TiO_2 mesoporous solar cells: working together with a common hole carrier of cobalt complexes. Chem Comm 2010;46:8788–90.
[40] Lee HJ, Bang J, Park J, Kim S, Park S-M. Multilayered semiconductor (CdS/CdSe/ZnS)-sensitized TiO_2 mesoporous solar cells: all prepared by successive ionic layer adsorption and reaction processes. Chem Mater 2010;22:5636–43.
[41] Lee HJ, Yum J-H, Leventis HC, Zakeeruddin SM, Haque SA, Chen P, Seok SI, Gratzel M, Nazeeruddin MK. CdSe quantum dot-sensitized solar cells exceeding efficiency 1% at full-sun intensity. J Phys Chem C 2008;112:11600–8.
[42] Lee HJ, Wang M, Chen P, Gamelin DR, Zakeeruddin SM, Gratzel M, Nazeeruddin MK. Efficient CdSe QUantum Dot-sensitized Solar Cells Prepared by an Improved Successive Ionic Layer Adsorption and Reaction Process. Nano Lett 2009;9:4221–7.
[43] Mora-Sero I, Gimenez S, Moehl T, Fabregat-Santiago F, Lana-Villareal T, Go'mez R, Bisquert J. Factors determining the photovoltaic performance of a CdSe quantum dot sensitized solar cell: the role of the linker molecule and of the counter electrode. Nanotechnology 2008;19:424007. http://dx.doi.org/10.1088/0957-4484/19/42/424007.
[44] Chen J, Li C, Zhao DW, Lei W, Zhang Y, Cole MT, Chu DP, Wang BP, Cui YP, Sun XW, Milne WI. A quantum dot sensitized solar cell based on vertically aligned carbon nanotube templated ZnO arrays. Electrochem Commun 2010;12:1432–5.
[45] Chen J, Li C, Song JL, Sun XW, Lei W, Deng WO. Bilayer ZnO nanostructure fabricated by chemical bath and its application in quantum dot sensitized solar cell. Appl Surf Sci 2009;255:7508–11.
[46] Chen J, Zhao DW, Song JL, Sun XW, Deng WQ, Liu XW, Lei W. Directly assembled CdSe quantum dots on TiO_2 in aqueous solution by adjusting pH value for quantum dot sensitized solar cells. Electrochem Commun 2009;11:2265–7.
[47] Chen J, Wu J, Lei W, Song JL, Deng WQ, Sun XW. Co-sensitized quantum dot solar cell based on ZnO nanowire. Appl Surf Sci 2010;256:7438–41.
[48] Chen J, Song JL, Sun XW, Deng WO, Jiang CY, Lei W, Huang JH, Liu RS. An oleic acid-capped CdSe quantum-dot sensitized solar cell. Appl Phys Lett 2009;94:153115. http://dx.doi.org/10.1063/1.3117221.
[49] Chen J, Lei W, Deng WQ. Reduced charge recombination in a co-sensitized quantum dot solar cell with two different sizes of CdSe quantum dot. Nanoscale 2011;3:674–7.
[50] Chen J, Lei W, Li C, Zhang Y, Cui Y, Wang B, Deng W. Flexible quantum dot sensitized solar cell by electrophoretic deposition of CdSequantum dots on ZnO nanorods. Phys Chem Chem Phys 2011;13:13182–4.
[51] Tian J, Gao R, Zhang Q, Zhang S, Li Y, Lan J, Qu X, Cao G. Enhanced performance of CdS/CdSe quantum dot cosensitized solar cells via homogeneous distribution of quantum dots in TiO_2 film. J Phys Chem 2012;116:18655–62.

[52] Radich JG, Dwyer R, Kamat PV. Cu_2S reduced graphene oxide composite for high-efficiency quantum dot solar cells. Overcoming the redox limitations of S_2^-/S_n^{2-} at the counter electrode. J Phys Chem Lett 2011;2:2453–60.

[53] Leschkies KS, Divakar R, Basu J, Enache-Pommer E, Boercker JE, Carter CB, Kortshagen UR, Norris DJ, Aydil ES. Photosensitization of ZnO nanowires with CdSe quantum dots for photovoltaic devices. Nano Lett 2007;7:1793–8.

[54] Li L, Yang X, Gao J, Tian H, Zhao J, Hagfeldt A, Sun L. Highly efficient CdS quantum dot-sensitized solar cells based on a modified polysulfide electrolyte. J Am Chem Soc 2011;133:8458–60.

[55] Diguna LJ, Shen Q, Kobayashi J, Toyoda T. High efficiency of CdSe quantum-dot-sensitized TiO_2 inverse opal solar cells. Appl Phys Lett 2007;91:023116. http://dx.doi.org/10.1063/1.2757130.

[56] Chong L-W, Chien H-T, Lee Y-L. Assembly of CdSe onto mesoporous TiO_2 films induced by a self-assembled monolayer for quantum dot-sensitized solar cell applications. J Power Sources 2010;195:5109–13.

[57] Deng M, Zhang Q, Huang S, Li D, Luo Y, Shen Q, Toyoda T, Meng Q. Low-Cost Flexible Nano-Sulfide/Carbon Composite Counter Electrode for Quantum-Dot-Sensitized Solar Cell. Nano Res Lett 2010;5:986–90.

[58] Li M, Liu Y, Wang H, Shen H, Zhao W, Huang H, Liang C. CdS/CdSe cosensitized oriented single-crystalline TiO_2 nanowire array for solar cell application. J Appl Phys 2010;108:094304. http://dx.doi.org/10.1063/1.3503409.

[59] Samadpour M, Boix PP, Gimenez S, Zad AI, Taghavinia N, Mora-Sero I, Bisquert J. Fluorine treatment of TiO_2 for enhancing quantum dot sensitized solar cell performance. J Phys Chem C 2011;115:14400–7.

[60] Seol M, Kim H, Tak Y, Yong K. Novel nanowire array based highly efficient quantum dot sensitized solar cell. Chem Commun 2010;46:5521–3.

[61] Hossain MA, Jennings JR, Shen C, Pan JH, Koh ZY, Mathews N, Wang Q. CdSe-sensitized mesoscopic TiO_2 solar cells exhibiting >5% efficiency: redundancy of CdS buffer layer. J Mater Chem 2012;22:16235–42.

[62] Hossain MF, Biswas S, Takahashi T. Study of CdS-sensitized solar cells, prepared by ammonia-free chemical bath technique. Thin Solid Films 2009;518:1599–602.

[63] Hossain MF, Biswas S, Zhang ZH, Takahashi T. Bubble-like CdSe nanoclusters sensitized TiO_2 nanotube arrays for improvement in solar cell. Photochem Photobiol A: Chem 2011;217:68–75.

[64] Yeh M-H, Lee C-P, Chou C-Y, Lin L-Y, Wei H-Y, Chu C-W, Vittal R, Ho K-C. Conducting polymer-based counter electrode for a quantum-dot-sensitized solar cell (QDSSC) with a polysulfide electrolyte. Electrochim Acta 2011;57:277–84.

[65] Guijarro NS, Shen Q, Gimenez S, Mora-Sero I, Bisquert J, Lana-Villarreal T, Toyoda T, Go´mez R. Direct correlation between ultrafast injection and photoanode performance in quantum dot sensitized solar cells. J Phys Chem 2010;114:22352–60.

[66] Niitsoo O, Sarkar SK, Pejoux C, Ruhle S, Cahen D, Hodes G. Chemical bath deposited CdS/CdSe-sensitized porous TiO_2 solar cells. J Photochem Photobio A: Chem 2006;181:306–13.

[67] Sudhagar P, Ramasamy E, Cho W-H, Lee J, Kang YS. Robust mesocellular carbon foam counter electrode for quantum-dot sensitized solar cells. Electrochem Comm 2011;13:34–7.

[68] Sudhagar P, Jung JH, Park S, Sathyamoorthy R, Ahn H, Kang YS. Self-assembled CdS quantum dots-sensitized TiO_2 nanospheroidal solar cells: structural and charge transport analysis. Electrochim Acta 2009;55:113–7.

[69] Sudhagar P, Jung JH, Park S, Lee Y-G, Sathyamoorthy R, Kang YS, Ahn H. The performance of coupled (CdS: cdse) quantum dot-sensitized TiO_2 nanofibrous solar cells. Electrochem Commun 2009;11:2220–4.

[70] Santra PK, Kamat PV. Mn-Doped Quantum Dot Sensitized Solar Cells: a Strategy to Boost Efficiency over 5%. J Am Chem Soc 2012;134:2508–11.

[71] Shen Q, Yamada A, Tamura S, Toyoda T. CdSe quantum dot-sensitized solar cell employing TiO_2 nanotube working-electrode and Cu_2S counter-electrode. Appl Phys Lett 2010;97:123107. http://dx.doi.org/10.1063/1.3491245.

[72] Shen Q, Kobayashi J, Diguna LJ, Toyoda T. Effect of ZnS coating on the photovoltaic properties of CdSe quantum dot-sensitized solar cells. J Appl Phys 2008;103:084304. http://dx.doi.org/10.1063/1.2903059.

[73] Zhang Q, Chen G, Yang Y, Shen X, Zhang Y, Li C, Yu R, Luo Y, Li D, Meng Q. Toward highly efficient CdS/CdSe quantum dots-sensitized solar cells incorporating ordered photoanodes on transparent conductive substrates. Phys Chem Chem Phys 2012;14:6479–86.

[74] Zhang Q, Guo X, Huang X, Huang S, Li D, Luo Y, Shen Q, Toyoda T, Meng Q. Highly efficient CdS/CdSe-sensitized solar cells controlled by the structural properties of compact porous TiO_2 photoelectrodes. Phys Chem Chem Phys 2011;13:4659–67.

[75] Zhang Q, Zhang Y, Huang S, Huang X, Luo Y, Meng Q, Li D. Application of carbon counterelectrode on CdS quantum dot-sensitized solar cells (QDSSCs). Electrochem Comm 2010;12:327–30.

[76] Cheng S, Fu W, Yang H, Zhang L, Ma J, Zhao H, Sun M, Yang L. Photoelectrochemical Performance of Multiple Semiconductors (CdS/CdSe/ZnS) Cosensitized TiO_2 Photoelectrodes. J Phys Chem C 2012;116:2615–21.

[77] Gimenez S, Mora-Sero I, Macor L, Guijarro N, Lana-Villarreal T, Go'mez R, Diguna LJ, Shen Q, Toyoda T, Bisquert J. Improving the performance of colloidal quantum-dot-sensitized solar cells. Nanotechnology 2009;20:295204. http://dx.doi.org/10.1088/0957-4484/20/29/295204.

[78] Greenwald S, Rühle S, Shalom M, Yahav S, Zaban A. Unpredicted electron injection in CdS/CdSe quantum dot sensitized ZrO_2 solar cells. Phys Chem Chem Phys 2011;13:19302–6.

[79] Huang S, Zhang Q, Huang X, Guo X, Deng M, Li D, Luo Y, Shen Q, Toyoda T, Meng Q. Fibrous CdS/CdSe quantum dot co-sensitized solar cells based on ordered TiO_2 nanotube arrays. Nanotechnology 2010;21:375201. http://dx.doi.org/10.1088/0957-4484/21/37/375201.

[80] Sun S, Gao L, Liu Y, Sun J. Assembly of CdSe nanoparticles on graphene for low-temperature fabrication of quantum dot sensitized solar cell. Appl Phys Lett 2011;98:093112. http://dx.doi.org/10.1063/1.3558732.

[81] Rawal SB, Sung SD, Moon S-Y, Shin Y-J, Lee WI. Optimization of CdS layer on ZnO nanorod arrays for efficient CdS/CdSe co-sensitized solar cell. Mater Lett 2012;82:240–3.

[82] Jung SW, Kim J-H, Kim H, Choi C-J, Ahn K-S. ZnS overlayer on in situ chemical bath deposited CdS quantum dot-assembled TiO_2 films for quantum dot-sensitized solar cells. Curr Appl Phys 2012;12:1459–64.

[83] Lin S-C, Lee Y-L, Chang C-H, Shen Y-J, Yang Y-M. Quantum-dot-sensitized solar cells: assembly of CdS-quantum-dots coupling techniques of self-assembled monolayer and chemical bath deposition. Appl Phys Lett 2007;90:143517. http://dx.doi.org/10.1063/1.2721373.

[84] Fan S-Q, Kim D, Kim J-J, Jung DW, Kang SQ, Ko J. Highly efficient CdSe quantum-dot-sensitized TiO_2 photoelectrodes for solar cell applications. Electrochem Commun 2009;11:1337–9.

[85] Lopez-Luke T, Wolcott A, Xu L-P, Chen S, Wen Z, Li J, Rosa EDL, Zhang JZ. Nitrogen-doped and CdSe Quantum-dot-sensitized nanocrystalline TiO_2 films for solar energy conversion applications. J Phys Chem C 2008;112:1282–92.

[86] Shu T, Xiang P, Zhou Z-M, Wang H, Liu G-H, Han H-W, Zhao Y-D. Mesoscopic nitrogen-doped TiO_2 spheres for quantum dot-sensitized solar cells. Electrochim Acta 2012;68:166–71.

[87] Zeng T, Tao H, Sui X, Zhou X, Zhao X. Growth of free-standing TiO_2 nanorod arrays and its application in CdS quantum dots-sensitized solar cells. Chem Phys Lett 2011;508:130–3.

[88] Zewdu T, Clifford JN, Hernandez JP, Palomares E. Photo-induced charge transfer dynamics in efficient TiO_2/CdS/CdSe sensitized solar cells. Energy Environ Sci 2011;4:4633–8.

[89] Gonzalez-Pedro V, Xu X, Mora-Sero I, Bisquert J. Modeling high-efficiency quantum dot sensitized solar cells. ACS Nano 2010;4:5783–90.

[90] Jovanovski V, Gonzalez-Pedro V, Gimenez S, Azaceta E, Cabanero G, Grande H, Tena-Zaera R, Mora-Sero I, Bisquert J. A sulfide/polysulfide-based ionic liquid electrolyte for quantum dot-sensitized solar cells. J Am Chem Soc 2011;133:20156–9.

[91] Jang W, Nursanto EB, Kim J, Park SJ, Min BK, Yoo K-P. Liquid carbon dioxide coating of CdS quantum-dots on mesoporous TiO_2 film for sensitized solar cell applications. J Supercrit Fluids 2012;70:40–7.

[92] Lee W, Min SK, Dhas V, Ogale SB, Han S-H. Chemical bath deposition of CdS quantum dots on vertically aligned ZnO nanorods for quantum dots-sensitized solar cells. Electrochem Comm 2009;11:103–6.

[93] Lee W, Kwak W-C, Min SK, Lee J-C, Chae W-S, Sung Y-M, Han S-H. Spectral broadening in quantum dots-sensitized photoelectrochemical solar cells based on CdSe and Mg-doped CdSe nanocrystals. Electrochem Comm 2008;10:1699–702.

[94] Lee WJ, Kang SH, Min SK, Sung Y-E, Han S-H. Co-sensitization of vertically aligned TiO_2 nanotubes with two different sizes of CdSe quantum dots for broad spectrum. Electrochem Comm 2008;10:1579–82.

[95] Huang X, Huang S, Zhang Q, Guo X, Li D, Luo Y, Shen Q, Toyoda T, Meng Q. A flexible photoelectrode for CdS/CdSe quantum dot-sensitized solar cells (QDSSCs). Chem Comm 2011;47:2664–6.

[96] Song X, Wang M, Shi Y, Deng J, Yang Z, Yao X. In situ hydrothermal growth of CdSe(S) nanocrystals on mesoporous TiO_2 films for quantum dot-sensitized solar cells. Electrochim Acta 2012;81:260–7.

[97] Gao X-F, Li H-B, Sun W-T, Chen Q, Tang F-Q, Peng L-M. CdTe quantum dots-sensitized TiO_2 nanotube array photoelectrodes. J Phys Chem C 2009;113:7531–5.

[98] Yu X-Y, Lei B-X, Kuang D-B, Su C-Y. Highly efficient CdTe/CdS quantum dot sensitized solar cells fabricated by a one-step linker assisted chemical bath deposition. Chem Sci 2011;2:1396–400.

[99] Yu X-Y, Lei B-X, Kuang D-B, Su C-Y. High performance and reduced charge recombination of CdSe/CdS quantum dot-sensitized solar cells. J Mater Chem 2012;22:12058–63.

[100] Lai Y, Lin Z, Zheng D, Chi L, Du R, Lin C. CdSe/CdS quantum dots co-sensitized TiO_2 nanotube array photoelectrode for highly efficient solar cells. Electrochim Acta 2012;79:175–81.

[101] Tachibana Y, Umekita K, Otsuka Y, Kuwabata S. Performance improvement of CdS quantum dots sensitized TiO_2 solar cells by introducing a dense TiO_2 blocking layer. J Phys D: Appl Phys 2008;41:102002. http://dx.doi.org/10.1088/0022-3727/41/10/102002.

[102] Zhang Y, Zhu J, Yu X, Wei J, Hu L, Dai S. The optical and electrochemical properties of CdS/CdSe co-sensitized TiO_2 solar cells prepared by successive ionic layer adsorption and reaction processes. Sol Energy 2012;86:964–71.

[103] Lee YH, Im SY, Lee J-H, Seok SI. Porous CdS-sensitized electrochemical solar cells. Electrochim Acta 2011;56:2087–91.

[104] Shen Y-J, Lee Y-L. Assembly of CdS quantum dots onto mesoscopic TiO_2 films for quantum dot-sensitized solar cell applications. Nanotechnology 2008;19:045602. http://dx.doi.org/10.1088/0957-4484/19/04/045602.

[105] Lee Y-L, Chang C-H. Efficient polysulfide electrolyte for CdS quantum dot-sensitized solar cells. J Power Sources 2008;185:584–8.

[106] Lee Y-L, Huang B-M, Chien H-T. Highly efficient CdSe-sensitized TiO_2 photoelectrode for quantum-dot-sensitized solar cell applications. Chem Mater 2008;20:6903–5.

[107] Lee Y-L, Lo Y-S. Highly efficient quantum-dot-sensitized solar cell based on co-sensitization of CdS/CdSe. Adv Funct Mater 2009;9:604–9.

[108] Liu Z, Miyauchi M, Uemura Y, Cui Y, Hara K, Zhao Z, Sunahara K, Furube A. Enhancing the performance of quantum dots sensitized solar cell by SiO_2 surface coating. Appl Phys Lett 2010;96:233107. http://dx.doi.org/10.1063/1.3447356.

[109] Ning Z, Yuan C, Tian H, Fu Y, Li L, Sun L, Agren H. Type-II colloidal quantum dot sensitized solar cells with a thiourea based organic redox couple. J Mater Chem 2012;22:6032–7.
[110] Ning Z, Tian H, Yuan C, Fu Y, Qin H, Sun L, Agren H. Solar cells sensitized with type-II ZnSe–CdS core/shell colloidal quantum dots. Chem Comm 2011;47:1536–8.
[111] Yang Z, Chang H-T. CdHgTe and CdTe quantum dot solar cells displaying an energy conversion efficiency exceeding 2%. Sol Energy Mater Sol Cells 2010;94:2046–51.
[112] Yang Z, Chen C-Y, Liu C-W, Chang H-T. Electrocatalytic sulfur electrodes for CdS/CdSe quantum dot-sensitized solar cells. Chem Commun 2010;46:5485–7.
[113] Yu Z, Zhang Q, Qin D, Luo Y, Li D, Shen Q, Toyoda T, Meng Q. Highly efficient quasi-solid-state quantum-dot-sensitized solar cell based on hydrogel electrolytes. Electrochem Commun 2010;12:1776–9.
[114] Ip AH, Thon SM, Hoogland S, Voznyy O, Zhitomirsky D, Debnath R, Levina L, Rollny LR, Carey GH, Fischer A, Kemp KW, Kramer IJ, Ning Z, Labelle AJ, Chou KW, Amassian A, Sargent EH. Hybrid passivated colloidal quantum dot solids. Nat Nanotechnol 2012;7:577–82.
[115] Cai B, Xing Y, Yang Z, Zhang W-H, Qiu J. High performance hybrid solar cells sensitized by organolead halide perovskites. Energy Environ Sci 2013;6:1480–5.
[116] Lim CS, Im SH, Kim JH, Chang JA, Lee YH, Seok SI. Enhancing the device performance of Sb_2S_3-sensitized heterojunction solar cells by embedding Au nanoparticles in the hole-conducting polymer layer. Phys Chem Chem Phys 2012;14:3622–6.
[117] Chi C-F, Chen P, Lee Y-L, Liu IP, Chou S-C, Zhang X-L, Bach U. Surface modifications of CdS/CdSe co-sensitized TiO_2 photoelectrodes for solid-state quantum-dot-sensitized solar cells. J Mater Chem 2011;21:17534–40.
[118] Bi D, Haggman L, Boschloo G, Yang L, Johansson EMJ, Hagfeldt A. Using a two-step deposition technique to prepare perovskite ($CH_3NH_3PbI_3$) for thin film solar cells based on ZrO_2 and TiO_2 mesostructures. RSC Adv 2013;3:18762–6.
[119] Bi D, Yang L, Boschloo G, Hagfeldt A, Johansson EMJ. Effect of different hole transport materials on recombination in $CH_3NH_3PbI_3$ perovskite-sensitized mesoscopic solar cells. J Phys Chem Lett 2013;4:1532–6.
[120] Edri E, Kirmayer S, Cahen D, Hodes G. High open-circuit voltage solar cells based on organic–inorganic lead bromide perovskite. J Phys Chem Lett 2013;4:897–902.
[121] Xu F, Benavides J, Ma X, Cloutier SG. Interconnected TiO_2 nanowire networks for PbS quantum dot solar cell applications. J Nanotechnol 2012;6:709031. http://dx.doi.org/10.1155/2012/709031.
[122] Yue G, Wu J, Xiao Y, Lin J, Huang M, Lan Z, Fan L. CdTe quantum dots-sensitized solar cells featuring PCBM/P3HT as hole transport material and assistant sensitizer provide 3.40% efficiency. Electrochim Acta 2012;85:182–6.
[123] Zhai G, Church CP, Breeze AJ, Zhang D, Alers GB, Carter SA. Quantum dot $PbS_{0.9}Se_{0.1}/TiO_2$ heterojunction solar cells. Nanotechnology 2012;23:405401. http://dx.doi.org/10.1088/0957-4484/23/40/40540.
[124] Lee H, Leventis HC, Moon S-J, Chen P, Ito S, Haque SA, Torres T, Nuesch F, Geiger T, Zakeeruddin SM, Gratzel M, Nazeeruddin MK. PbS and CdS quantum dot-sensitized solid-state solar cells: “old Concepts, New Results”. Adv Func Mater 2009;19:2735–42.
[125] Kim HS, Lee CR, Im JH, Lee KB, Moehl T, Marchioro A, Moon SJ, Humphry-Baker R, Yum JH, Moser JE, Gratzel M, Park NG. Lead iodide perovskite sensitized all-solid-state submicron thin film mesoscopic solar cell with efficiency exceeding 9%. Sci Rep 2012;2:591. http://dx.doi.org/10.1038/srep00591.
[126] Kim HS, Lee JW, Yantara N, Boix PP, Kulkarni SA, Mhaisalkar S, Gratzel M, Park NG. High efficiency solid-state sensitized solar cell-based on submicrometer rutile TiO_2 nanorod and $CH_3NH_3PbI_3$ perovskite sensitizer. Nano Lett 2013;13:2412–7.
[127] Barcelo I, Campina JM, Lana-Villarreal T, Gomez R. A solid-state CdSe quantum dot sensitized solar cell based on a quaterthiophene as a hole transporting material. Phys Chem Chem Phys 2012;14:5801–7.
[128] Kramer IJ, Zhitomirsky D, Bass JD, Rice PM, Topuria T, Krupp L, Thon SM, Ip AH, Debnath R, Kim HC, Sargent EH. Ordered nanopillar structured electrodes for depleted bulk heterojunction colloidal quantum dot solar cells. Adv Mater 2012;24:2315–9.
[129] Burschka J, Pellet N, Moon SJ, Humphry-Baker R, Gao P, Nazeeruddin MK, Grätzel M. Sequential deposition as a route to high-performance perovskite-sensitized solar cells. Nature 2013;499:316–9.
[130] Qian J, Liu QS, Li G, Jiang KJ, Yang LM, Song Y. P3HT as hole transport material and assistant light absorber in CdS quantum dots-sensitized solid-state solar cells. Chem Comm 2011;47:6461–3.
[131] Qiu J, Qiu Y, Yan K, Zhong M, Mu C, Yan H, Yang S. All-solid-state hybrid solar cells based on a new organometal halide perovskite sensitizer and one-dimensional TiO_2 nanowire arrays. Nanoscale 2013;5:3245–8.
[132] Tang J, Kemp KW, Hoogland S, Jeong KS, Liu H, Levina L, Furukawa M, Wang X, Debnath R, Cha D, Chou KW, Fischer A, Amassian A, Asbury JB, Sargent EH. Colloidal-quantum-dot photovoltaics using atomic-ligand passivation. Nat Mater 2011;10:765–71.
[133] Chang JA, Rhee JH, Im SH, Lee YH, Kim HJ, Seok SI, Nazeeruddin MK, Gratzel M. High-performance nanostructured inorganic–organic heterojunction solar cells. Nano Lett 2010;10:2609–12.
[134] Chang JA, Im SH, Lee YH, Kim HJ, Lim CS, Heo JH, Seok SI. Panchromatic photon-harvesting by hole-conducting materials in inorganic–organic heterojunction sensitized-solar cell through the formation of nanostructured electron channels. Nano Lett 2012;12:1863–7.
[135] Heo JH, Im SH, Noh JH, Mandal TN, Lim C-S, Chang JA, Lee YH, Kim H-J, Sarkar A, Nazeeruddin MK, Gratzel M, Seok SI. Efficient inorganic–organic hybrid heterojunction solar cells containing perovskite compound and polymeric hole conductors. Nat Photon 2013;7:486–91.
[136] Noh JH, Im SH, Heo JH, Mandal TN, Seok SI. Chemical management for colorful, efficient, and stable inorganic–organic hybrid nanostructured solar cells. Nano Lett 2013;13:1764–9.
[137] Ball JM, Lee MM, Hey A, Snaith HJ. Low-temperature processed *meso*-superstructured to thin-film perovskite solar cells. Energy Environ Sci 2013;6:1739–43.
[138] Tsujimoto K, Nguyen D-C, Ito S, Nishino H, Matsuyoshi H, Konno A, Kumara GRA, Tennakone K. TiO_2 surface treatment effects by Mg^{2+}, Ba^{2+}, and Al^{3+} on Sb_2S_3 extremely thin absorber solar cells. J Phys Chem C 2012;116:13465–71.
[139] Jeong KS, Tang J, Liu H, Kim J, Schaefer AW, Kemp K, Levina L, Wang X, Hoogland S, Debnath R, Brzozowski L, Sargent EH, Asbury JB. Enhanced mobility-lifetime products in PbS colloidal quantum dot photovoltaics. ACS Nano 2012;6:89–99.
[140] Etgar L, Yanover D, Capek RK, Vaxenburg R, Xue Z, Liu B, Nazeeruddin MK, Lifshitz E, Gratzel M. Core/shell PbSe/PbS QDs TiO_2 heterojunction solar cell. Adv Funct Mater 2013;23:2736–41.
[141] Etgar L, Gao P, Xue Z, Peng Q, Chandiran AK, Liu B, Nazeeruddin MK, Gratzel M. Mesoscopic $CH_3NH_3PbI_3/TiO_2$ heterojunction solar cells. J Am Chem Soc 2012;134:17396–9.
[142] Etgar L, Zhang W, Gabriel S, Hickey SG, Nazeeruddin MK, Eychmuller A, Liu B, Gratzel M. High efficiency quantum dot heterojunction solar cell using anatase (001) TiO_2 nanosheets. Adv Mater 2012;24:2202–6.
[143] Lee MM, Teuscher J, Miyasaka T, Murakami TN, Snaith HJ. Efficient hybrid solar cells based on meso-superstructured organometal halide perovskites. Science 2012;338:643–7.
[144] Balis N, Dracopoulos V, Stathatos E, Boukos N, Lianos P. A solid-state hybrid solar cell made of nc-TiO_2, CdS quantum dots, and P3HT with 2-Amino-1-methylbenzimidazole as an Interface Modifier. J Phys Chem C 2011;115:10911–6.
[145] Dowland S, Lutz T, Ward A, King SP, Sudlow A, Hill MS, Molloy KC, Haque SA. Direct growth of metal sulfide nanoparticle networks in solid-state polymer films for hybrid inorganic–organic solar cells. Adv Mater 2011;23:2739–44.
[146] Kim S, Im SH, Kang M, Heo JH, Seok SI, Kim SW, Mora-Sero I, Bisquert J. Air-stable and efficient inorganic–organic heterojunction solar cells using PbS colloidal quantum dots co-capped by 1-dodecanethiol and oleic acid. Phys Chem Chem Phys 2012;14:14999–5002.
[147] Nezu S, Larramona G, Chone´ C, Jacob A, Delatouche B, Pe´re´ D, Moisan C. Light soaking and gas effect on nanocrystalline $TiO_2/Sb_2S_3/CuSCN$ photovoltaic cells following extremely thin absorber concept. J Phys Chem C 2010;114:6854–9.
[148] Im SH, Kim H-J, Kim SW, Kim S-W, Seok SI. All solid state multiply layered PbS colloidal quantum-dot-sensitized photovoltaic cells. Energy Environ Sci 2011;4:4181–6.
[149] Moon SJ, Itzhaik Y, Yum JH, Zakeeruddin SM, Hodes G, Gratzel M. Sb_2S_3-based mesoscopic solar cell using an organic hole conductor. J Phys Chem Lett 2010;1:1524–7.
[150] Fukumoto T, Moehl T, Niwa Y, Nazeeruddin MK, Gratzel M, Etgar L. Effect of interfacial engineering in solid-state nanostructured Sb_2S_3 heterojunction solar cells. Adv Energy Mater 2013;3:29–33.
[151] Brennan TP, Ardalan P, Lee H-B-R, Bakke JR, Ding IK, McGehee MD, Bent SF. Atomic layer deposition of CdS quantum dots for solid-state quantum dot sensitized solar cells. Adv Energy Mater 2011;1:1169–75.
[152] Itzhaik Y, Niitsoo O, Page M, Hodes G. Sb_2S_3-sensitized nanoporous TiO_2 solar cells. J Phys Chem C 2009;113:4254–6.
[153] Lee YH, Im SH, Chang JA, Lee J-H, Seok SI. CdSe-sensitized inorganic-organic heterojunction solar cells: the effect of molecular dipole interface modification and surface passivation. Org Electr 2012;13:975–9.
[154] Chen Z, Zhang H, Yu W, Li Z, Hou J, Wei H, Yang B. Inverted hybrid solar cells from aqueous materials with a PCE of 3.61%. Adv Energy Mater 2013;3:433–7.
[155] Tabachnick BG, Fidell LS. Using multivariate statistics, 4th edition. Boston, MA: Allyn and Bacon; 2001.
[156] Menard S. Applied logistic regression analysis: sage university series on quantitative applications in the social sciences. Thousand Oaks, CA: Sage Publications; 1995.
[157] Huber E, Stephens JD. Political parties and public pensions: a quantitative analysis. Acta Sociol 1993;36:309–25.
[158] BJA Colton, Bower KM. Some misconceptions about R-squared. Int Soc Six Sigma Prof Extraordinary Sense 2002;3(2):20–2.
[159] Gao B, Shen C, Zhang B, Zhang M, Yuan S, Yang Y, Chen G, Green synthesis of highly efficient CdSe quantum dots for quantum-dots-sensitized solar cells. J. Appl. Phys. vol. 214(115), p. 193104.
[160] Kim S-K, Gopi CVVM, Lee J-C, Kim H-J. Enhanced performance of branched TiO_2 nanorod based Mn-doped CdS and Mn-doped CdSe quantum dot-sensitized solar cell. J Appl Phys 2015;117:163104.
[161] Badawi A, Al-Hosiny N, Abdallah1 S, Talaat H. Tuning photocurrent response through size control of CdSe quantum dots sensitized solar cells. Mater Sci-Pol 2013;31(1):6–13.
[162] Badawi Ali, Al-Hosiny N, Abdallah Said, Negm S, Talaat H. Tuning photocurrent response through size control of CdTe quantum dots sensitized solar cells. Sol Energy 2013;88:137–43.
[163] Wang Baoyuan, Ding Hao, Hu Yunxia, Zhou Hai, Wang Shuqiang, Wang Tian, Liu Rong, Zhang Jun, Wang Xina, Wang Hao. Power conversion efficiency enhancement of various size CdS quantum dots and dye cosensitized solar cells. Int J Hydrog Energy 2013;38:16733–9.
[164] Justin Raj C, Karthick SN, Hemalatha KV, Kima Hee-Je, Prabakar K. Highly efficient ZnO porous nanostructure for CdS/CdSe quantum dot sensitized solar

cell. Thin Solid Films 2013;548:636–40.
[165] Chen Hong-Yan, Lin Ling, Yu Xiao-Yun, Qiu Kang-Qiang, Lü Xian-Yong, Kuang Dai-Bin, Su Cheng-Yong. Dextran based highly conductive hydrogel polysulfide electrolyte for efficient quasi-solid-state quantum dot-sensitized solar cells. Electrochim Acta 2013;92:117–23.
[166] Li Dong-Mei, Cheng Lu-Yao, Zhang Yi-Duo, Zhang Quan-Xin, Huang Xiao-Ming, Luo Yan-Hong, Meng Qing-Bo. Development of Cu2S/carbon composite electrode for CdS/CdSe quantum dot sensitized solar cell modules. Sol Energy 2014;120:454–61.
[167] Selopal Gurpreet S, Concina Isabella, Milan Riccardo, Natile Marta M, Sberveglieri Giorgio, Vomiero Alberto. Hierarchical self-assembled Cu2S nanostructures: fast and reproducible spray deposition of effective counter electrodes for high efficiency quantum dot solar cells. Nano Energy 2014;6:200–10.
[168] Thanh Tung Ha, Vinh Lam Quang, Dat Huynh Thanh. The dynamic resistance of CdS/CdSe/ZnS Co-sensitized TiO_2 solar cells. Braz J Phys 2014;44:746–52.
[169] Ayyaswamy Arivarasan, Ganapathy Sasikala, Alsalme Ali, Alghamdi Abdulaziz, Ramasamy Jayavel. Structural, optical and photovoltaic properties of co-doped CdTe QDs for quantum dots sensitized solar cells. Superlattices Microstruct 2015;88:634–44.
[170] Samadpour M, Rezanejade Bardajee G, Ghiasvand Gheysare S, Shafagh P. Transition metal doping for enhancing quantum dot sensitized solar cells performance. J Phys D: Appl Phys 2015;48:095101, [6pp].
[171] Huo Zhipeng, Tao Li, Wang Shimao, Wei Junfeng, Zhu Jun, Dong Weiwei, Liu Feng, Chen Shuanghong, Zhang Bing, Dai Songyuan. A novel polysulfide hydrogel electrolyte based on low molecular mass organogelator for quasi-solid-state quantum dot-sensitized solar cells. J Power Sources 2015;284:582–7.
[172] Qiao Wentao, Zhang Dafeng, Zhang Liwei, Kang Chaoyang. Post-thermal annealing for enhancing photovoltaic performance of CdS/CdSe quantum dot co-sensitized TiO_2 electrodes. J Alloy Compd 2016;658:697–702.
[173] Leahy K. Multicollinearity: when the solution is the problem. In: Olivia PR, editor. Data mining cookbook. New York: Wiley; 2000.
[174] Nevou L, Liverini V, Friedli P, Castellano F, Bismuto A, Sigg H, Gramm F, Müller E, Faist J. Current quantization in an optically driven electron pump based on self-assembled quantum dots. Nat Phys 2011;7:423–7.
[175] Yoffe AD. Semiconductor quantum dots and related systems: electronic, optical, luminescence and related properties of low dimensional systems. Adv Phys 2001;50(1):1–208.
[176] Kilina SV, Kilin DS, Prezhdo OV. Breaking the phonon bottleneck in pbse and cdse quantum dots: time-domain density functional theory of charge carrier relaxation. ACS Nano 2009;3:93–9.
[177] Nozik AJ. Quantum dot solar cells. Physica E 2002;14:115–20.
[178] Madrid AB, Hyeon-Deuk K, Habenicht BF, Prezhdo OV. Phonon-induced dephasing of excitons in semiconductor quantum dots: multiple exciton generation, fission, and luminescence. ACS Nano 2009;3(9):2487–94.
[179] Ross RT, Nozik AJ. Efficiency of hot-carrier solar energy converters. J Appl Phys 1982;53:3813–8. http://dx.doi.org/10.1063/1.331124.
[180] Boudreaux DS, Williams F, Nozik AJ. Hot carrier injection at semiconductor-electrolyte junctions. J Appl Phys 1980;51:2158–63.
[181] Landsberg PT, Nussbaumer H, Willeke G. Band-band impact ionization and solar cell efficiency. J Appl Phys 1993;74:1451. http://dx.doi.org/10.1063/1.354886.
[182] Kolodinski S, Werner JH, Wittchen T, Queisser HJ. Quantum efficiencies exceeding unity due to impact ionization in silicon solar cells. Appl Phys Lett 1993;63:2405–7.
[183] Grätzel M. Review article photoelectrochemical cells. Nature 2001;414:338–44.
[184] Blanton SA, Leheny RL, Hines MA, Guyot-Sionnest P. Dielectric dispersion measurements of CdSe nanocrystal colloids: observation of a permanent dipole moment. Phys Rev Lett 1997;79:865–8.
[185] Schmidt ME, Blanton SA, Hines MA, Guyot-Sionnest P. Polar CdSe nanocrystals: implications for electronic structure. J Chem Phys 1997;106:5254–9.
[186] Tomasulo A, Ramakrishna MV. Quantum confinement effects in semiconductor clusters. Ii J Chem Phys 1996;105:3612–26.
[187] Pattantyus-Abraham AG, Kramer IJ, Barkhouse AR, Wang X, Konstantatos G, Debnath R, Levina L, Raabe I, Nazeeruddin MK, Grätzel M, Sargent EH. ACS Nano 2010;4:3374–80.
[188] Luther JM, Gao J, Lloyd MT, Semonin OE, Beard MC, Nozik AJ. Stability assessment on a 3% bilayer PbS/ZnO quantum dot heterojunction solar cell. Adv Mater 2010;22:3704–7.
[189] Chang L-Y, Lunt RR, Brown PR, Bulović V, Bawendi MG. Low-temperature solution-processed solar cells based on PbS colloidal quantum Dot/CdS heterojunctions. Nano Lett 2013;13:994–9.
[190] Lan X, Masala S, Sargent EH. Charge-extraction strategies for colloidal quantum dot photovoltaics. Nat Mater 2014;13:233–40.
[191] Nozik AJ, Boudreaux DS, Chance RR, Williams F. Advances. In: Wrighton M, editor. . Chemistry, 184. New York: ACS; 1980. p. 162.
[192] Williams FE, Nozik AJ. Solid-state perspectives of the photoelectrochemistry of semiconductor–electrolyte junctions. Nature 1984;312:21–7.
[193] Nozik AJ. Philos Trans R Soc Lond Ser A 1980;295:453–70.
[194] Barkhouse DAR, Pattantyus-Abraham AG, Levina L, Sargent EH. Thiols passivate recombination centers in colloidal quantum dots leading to enhanced photovoltaic device efficiency. ACS Nano 2008;2:2356–62.
[195] Kovalenko MV, Scheele M, Talapin DV. Colloidal nanocrystals with molecular metal chalcogenide surface ligands. Science 2009;324:1417–20.
[196] Law M, Luther JM, Song Q, Hughes BK, Perkins CL, Nozik AJ. Structural, optical, and electrical properties of PbSe nanocrystal solids treated thermally or with simple amines. J Am Chem Soc 2008;130:5974–85.
[197] Lee J-S, Kovalenko MV, Huang J, Chung DS, Talapin DV. Band-like transport, high electron mobility and high photoconductivity in all-inorganic nanocrystal arrays. Nat Nanotechnol 2011;6:348–52.
[198] Owen JS, Park J, Trudeau P-E, Alivisatos AP. Reaction chemistry and ligand exchange at cadmium–selenide nanocrystal surfaces. J Am Chem Soc 2008;130:12279–81.
[199] Talapin DV, Murray CB. PbSe nanocrystal solids for n- and p-channel thin film field-effect transistors. Science 2005;310:86–9.
[200] McDonald SA, Konstantatos G, Zhang S, Cyr PW, Klem EJD, Levina L, Sargent EH. Solution-processed PbS quantum dot infrared photodetectors and photovoltaics. Nat Mater 2005;4:138–42.
[201] Luther JM, Law M, Song Q, Perkins CL, Beard MC, Nozik AJ. Structural, optical, and electrical properties of self-assembled films of PbSe nanocrystals treated with 1,2-Ethanedithiol. ACS Nano 2008;2:271–80.
[202] Liu Y, Gibbs M, Puthussery J, Gaik S, Ihly R, Hillhouse HW, Law M. Dependence of carrier mobility on nanocrystal size and ligand length in PbSe nanocrystal solids. Nano Lett 2010;10:1960–9.
[203] Bang JH. Influence of nanoporous oxide substrate on the performance of photoelectrode in semiconductor-sensitized solar cells. Bull Korean Chem Soc 2012;33(12):4063–8.
[204] Tiwana P, Docampo P, Johnston MB, Snaith HJ, Herz LM. Electron mobility and injection dynamics in mesoporous ZnO, SnO_2, and TiO_2 films used in dye-sensitized solar cells. ACS Nano 2011;5:5158–66.
[205] Anta JA. Electron transport in nanostructured metal-oxide semiconductors. Curr Opin Colloid Interface Sci 2012;17:124–31.
[206] Hagfeldt A, Boschloo G, Sun L, Kloo L, Pettersson H. Dye-sensitized solar cells. Chem Rev 2010;110:6595–663.
[207] Grätzel M. Dye-sensitized solar cells. J Photochem Photobiol C 2003;4:145–53.
[208] Mora-Seroì I, Gimeìnez S, Fabregat-Santiago F, Goìmez R, Shen Q, Toyoda T, Bisquert J. Recombination in quantum dot sensitized solar cells. Acc Chem Res 2009;42:1848–57.
[209] Guijarro N, Shen Q, Gimeìnez S, Mora-Seroì I, Bisquert J, Lana-Villarreal T, Toyoda T, Goìmez R. Direct correlation between ultrafast injection and photoanode performance in quantum dot sensitized solar cells. J Phys Chem C 2010;114:22352–60.
[210] He H, Yang K, Wang N, Luo F, Chen H. Hydrogenated TiO_2 film for enhancing photovoltaic properties of solar cells and self-sensitized effect. J Appl Phys 2013;114:213505. http://dx.doi.org/10.1063/1.4832783.
[211] Liu YJ, Szeifert JM, Feckl JM, Mandlmeier B, Rathousky J, Hayden O, Fattakhova-Rohlfing D, Bein T. Niobium-doped titania nanoparticles: synthesis and assembly into mesoporous films and electrical conductivity. ACS Nano 2010;4:5373–81.
[212] Choi H, Kim J, Nahm C, Kim C, Nam S, Kang J, Lee B, Hwang T, Kang S, Choi DJ, Kim Y-H, Park B. The role of ZnO-coating-layer thickness on the recombination in CdS quantum-dot-sensitized solar cells. Nano Energy 2013;2:1218–24.
[213] Tsai C-W, Tong L-I, Wang C-H. Optimization of multiple responses using data envelopment analysis and response surface methodology. Tamkang J Sci Eng 2010;13(2):197–203.
[214] Khuri AI, Mukhopadhyay S. Response surface methodology. WIREs Comput Stat 2010;2:128–49.
[215] Brendel R, Werner JH, Queisser HJ. Thermodynamic efficiency limits for semiconductor solar cells with carrier multiplication. Sol Energy Mater Sol Cells 1996;41–42:419–25.